

An improved macroscale model for gas slip flow in porous media

Didier Lasseux^{1,†}, Francisco J. Valdés Parada² and Mark L. Porter³

¹CNRS, (Univ. Bordeaux, IPB, ENSAM) - I2M, UMR5295, Esplanade des Arts et Métiers, 33405 Talence, CEDEX, France

²Universidad Autónoma Metropolitana-Iztapalapa, Departamento de Ingeniería de Procesos e Hidráulica, Av. San Rafael Atlixco 186, 09340 Mexico D.F., Mexico

³Earth Systems Observations, MS D462, Los Alamos National Laboratory, Los Alamos, NM 85745, USA

(Received 25 August 2015; revised 30 July 2016; accepted 21 August 2016;
first published online 16 September 2016)

We report on a refined macroscopic model for slightly compressible gas slip flow in porous media developed by upscaling the pore-scale boundary value problem. The macroscopic model is validated by comparisons with an analytic solution on a two-dimensional (2-D) ordered model structure and with direct numerical simulations on random microscale structures. The symmetry properties of the apparent slip-corrected permeability tensor in the macroscale momentum equation are analysed. Slip correction at the macroscopic scale is more accurately described if an expansion in the Knudsen number, beyond the first order considered so far, is employed at the closure level. Corrective terms beyond the first order are a signature of the curvature of solid–fluid interfaces at the pore scale that is incompletely captured by the classical first-order correction at the macroscale. With this expansion, the apparent slip-corrected permeability is shown to be the sum of the classical intrinsic permeability tensor and tensorial slip corrections at the successive orders of the Knudsen number. All the tensorial effective coefficients can be determined from intrinsic and coupled but easy-to-solve closure problems. It is further shown that the complete form of the slip boundary condition at the microscale must be considered and an important general feature of this slip condition at the different orders in the Knudsen number is highlighted. It justifies the importance of slip-flow correction terms beyond the first order in the Knudsen number in the macroscopic model and sheds more light on the physics of slip flow in the general case, especially for large porosity values. Nevertheless, this new nonlinear dependence of the apparent permeability with the Knudsen number should be further verified experimentally.

Key words: low-Reynolds-number flows, porous media, rarefied gas flow

1. Introduction

The interest for studying slightly compressible gas slip flow in channels of characteristic dimension comparable to the gas mean free path at the pressure and temperature under consideration is tremendous for many applications that encompass

† Email address for correspondence: didier.lasseux@ensam.eu

gas flow in microchannels and nanofluidic systems (Porodnov *et al.* 1974; Harley *et al.* 1995; Karniadakis, Beskok & Aluru 2005; Cai, Sun & Boyd 2007), characterization of low permeable porous materials (Lasseux *et al.* 2011; Jannot & Lasseux 2012; Profice *et al.* 2012) involved in processes ranging from gas production (Darabi *et al.* 2012), gas or nuclear waste storage, filtration and separation (Chmielewski & Goren 1972), composite manufacturing (Zhang *et al.* 2009) among many others. Consequently, a great deal of interest may also be focused on the prediction and estimation of the coefficients governing the physics of gas transport at the macroscale. The emergence of powerful imaging methods together with the increase of computational capabilities make this prediction from direct numerical simulation, based upon images performed on a representative elementary volume (REV) of the porous structure at the microscale a realistic and promising approach to avoid sophisticated experiments (Ghaddar 1995; Nakashima & Watanabe 2002; deSocio & Marino 2006; Prodanović, Lindquist & Seright 2007).

To progress towards this goal, our purpose is to carefully derive an accurate macroscopic model for gas flow in homogeneous porous media in the slip regime. The existing model obtained so far in this context (Skjetne & Auriault 1999; Lasseux *et al.* 2014) is inaccurate. In fact, we show that the existing macroscopic slip correction filters out some important pore-scale topological information related to the curvature of solid–fluid interfaces, which can have significant impact in some circumstances at the macroscopic level. The model derived in this work avoids such a simplification and yields a macroscale model together with associated closures that are easy-to-solve boundary value problems defined at the microscale on a REV, which provide the required macroscopic coefficients.

The development proposed hereafter is organized as follows. The problem statement is presented first in §2 together with the main steps of the upscaling leading to the non-closed macroscopic form. The procedure to close the macroscopic momentum equation is reported in §§3.1 and 3.2 providing the closure problem that defines the apparent slip-corrected permeability, K_s , the non-intrinsic effective coefficient appearing in the macroscopic model. Validation of the upscaled model is presented in §3.3. Solutions obtained from direct numerical simulations (DNS) of incompressible slip flow performed on random two-dimensional (2-D) structures are used in the predictive macroscopic averaged model to identify K_s that is further compared to the solution of the closure problem. In addition, the analytic estimation of K_s is compared to the values obtained from numerical solutions of the closure over a periodic unit cell of the structure. In both cases, K_s depends nonlinearly on the Knudsen number at the macroscale, \overline{Kn} , based on the characteristic length scale within the fluid phase, a behaviour that can not be predicted from porous media slip-flow models reported so far (Skjetne & Auriault 1999; Lasseux *et al.* 2014).

In order to elucidate the nonlinearity and to obtain a macroscale model involving coefficients that are intrinsic to the micro-structure, an expansion in \overline{Kn} is provided in §4. Effective coefficients in this model correspond to the intrinsic permeability tensor at the zeroeth order and to slip-correction tensors at the successive higher orders in \overline{Kn} , all of them being obtained from the solution of coupled closure problems. This is detailed in §4.1. The existing Darcy–Klinkenberg model extensively used for gas slip flow in porous media, corresponds to the expansion up to the first order, together with an ideal gas law. In §4.2, it is shown that a more accurate description of the macroscopic behaviour, capturing the nonlinearity in \overline{Kn} previously observed, requires higher-order terms of the expansion. These terms are an explicit signature of the solid–fluid interface curvature that is not present in the first-order term. This is assessed

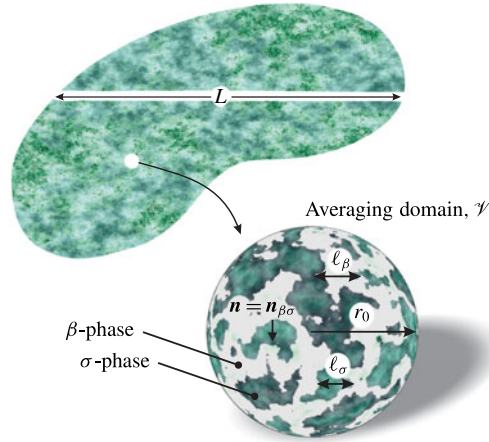


FIGURE 1. (Colour online) Averaging domain and characteristic lengths of the system.

in § 4.3, where important features of the slip boundary condition with respect to the successive orders of the expansion are reported, shedding more light on the physics of slip flow far beyond the application to porous media. Symmetry properties of the tensor \mathbf{K}_s are investigated in appendix A. Conclusions are drawn in § 5.

2. Problem statement and upscaling

The starting point of the analysis is the initial boundary value problem at the pore scale with characteristic length ℓ_β (see figure 1) describing the isothermal, Newtonian and slightly compressible flow of a barotropic fluid β occupying the sub-domain \mathcal{V}_β inside an averaging domain \mathcal{V} of radius r_0 .

We recall the problem statement as

$$\frac{\partial \rho_\beta}{\partial t} + \nabla \cdot (\rho_\beta \mathbf{v}_\beta) = 0 \quad \text{in } \mathcal{V}_\beta \tag{2.1a}$$

$$0 = -\nabla p_\beta + \mu_\beta \nabla^2 \mathbf{v}_\beta \quad \text{in } \mathcal{V}_\beta \tag{2.1b}$$

$$\rho_\beta = F(p_\beta) \quad \text{in } \mathcal{V}_\beta \tag{2.1c}$$

$$\text{B.C.1} \quad \mathbf{v}_\beta = -\xi \lambda_\beta (\mathbf{I} - \mathbf{nn}) \cdot (\mathbf{n} \cdot (\nabla \mathbf{v}_\beta + \nabla \mathbf{v}_\beta^T)) \quad \text{at } \mathcal{A}_{\beta\sigma} \tag{2.1d}$$

$$\text{B.C.2} \quad \mathbf{v}_\beta = \mathbf{f}(t) \quad \text{at } \mathcal{A}_{\beta e} \tag{2.1e}$$

$$\text{I.C.} \quad \rho_\beta = \rho_{\beta,0} \quad \text{when } t = 0. \tag{2.1f}$$

In these equations, ρ_β , \mathbf{v}_β and p_β are the density (of initial value $\rho_{\beta,0}$), velocity and pressure in the β -phase obeying the state equation (2.1c), μ_β is the dynamic viscosity, taken as a constant, λ_β is the mean free path, ξ is a parameter related to the tangential momentum accommodation coefficient, σ_v , given by $\xi = (2 - \sigma_v)/\sigma_v$ (Agrawal & Prabhu 2008; Selden *et al.* 2009). In practice, ξ ranges from approximately 1.3–1.7 (Suetin *et al.* 1973; Arkilic, Breuer & Schmidt 2001; Perrier *et al.* 2011). The unit normal vector at the solid–fluid interface $\mathcal{A}_{\beta\sigma}$, directed from the β - to the solid σ -phase, is denoted by \mathbf{n} while $\mathcal{A}_{\beta e}$ represents the entrance and exit surfaces of the β -phase at the boundaries of the averaging domain on which the fluid velocity is $\mathbf{f}(t)$. The first-order slip boundary condition expressed in (2.1d) and originally derived by

Navier and Maxwell (Maxwell 1879), includes the complete strain rate $(\nabla \mathbf{v}_\beta + \nabla \mathbf{v}_\beta^T)$. The $\nabla \mathbf{v}_\beta^T$ term plays an important role in general (Einzel, Panzer & Liu 1990; Panzer, Liu & Einzel 1992; Barber *et al.* 2004; Lockerby *et al.* 2004; Lasseux *et al.* 2014), although it has been often omitted for porous media flow (Skjetne & Auriault 1999; Pavan & Chastanet 2011). More physical insight will be provided into this boundary condition in § 4.2 below.

While writing the initial boundary value problem given by (2.1), a set of constraints were assumed that can be listed as

$$\frac{\rho_\beta}{\Delta\rho_\beta} \frac{v_\beta t_\rho^*}{\ell_\beta(1 + \xi Kn)} \frac{L_\rho}{\ell_\beta} \gg 1 \tag{2.2}$$

$$\frac{\rho_\beta}{\Delta\rho_\beta} \frac{1}{1 + \xi Kn} \left(\frac{L_\rho}{\ell_\beta}\right)^2 \gg 1 \tag{2.3}$$

$$\frac{\rho_\beta(1 + \xi Kn)\ell_\beta^2}{\mu_\beta t_v^*} \ll 1. \tag{2.4}$$

The first two constraints are required to neglect viscous terms related to compressible effects in the momentum equation whereas the last one is necessary to neglect the temporal acceleration; in both cases the comparisons are made with respect to the viscous diffusion term. In addition, to neglect the convective acceleration term, we require

$$Re = \frac{\rho_\beta \ell_\beta v_\beta}{\mu_\beta} \ll 1. \tag{2.5}$$

In the above constraints, which are easily met in practice and were thoroughly discussed in a recent article (Lasseux *et al.* 2014), v_β represents the order of magnitude of \mathbf{v}_β whereas L_ρ and t_ρ^* are the characteristic length and time scales over which ρ_β experiences significant variations $\Delta\rho_\beta$, $Kn = \lambda_\beta/\ell_\beta$ is the Knudsen number, which is assumed to remain smaller than approximately 0.1–0.4, characterizing the slip-flow regime in straight channels (Harley *et al.* 1995; Maurer *et al.* 2003). The left-hand side in the relationship (2.4) is nothing other than the frequency parameter of the flow with t_v^* being the characteristic time over which \mathbf{v}_β experiences significant variations and Re in (2.5) is the Reynolds number of the flow.

Upscaling of the problem given by (2.1) can be performed with the aid of the volume averaging method (Whitaker 1999) for which the intrinsic and superficial averages of any physical variable ψ_β are defined as

$$\langle \psi_\beta \rangle^\beta = \frac{1}{V_\beta} \int_{\mathcal{V}_\beta} \psi_\beta \, dV \tag{2.6}$$

$$\langle \psi_\beta \rangle = \varepsilon \langle \psi_\beta \rangle^\beta = \frac{1}{V} \int_{\mathcal{V}_\beta} \psi_\beta \, dV \tag{2.7}$$

ε denoting the porosity of the medium. The development of the averaged equations makes use of the averaging theorem (or Leibnitz rule) (Howes & Whitaker 1985) given by

$$\langle \nabla \psi_\beta \rangle = \nabla \langle \psi_\beta \rangle + \frac{1}{V} \int_{\mathcal{A}_{\beta\sigma}} \mathbf{n} \psi_\beta \, dA \tag{2.8}$$

along with the Reynolds theorem (Truesdell & Toupin 1960) and the classical decomposition (Gray 1975)

$$\psi_\beta = \langle \psi_\beta \rangle^\beta + \tilde{\psi}_\beta. \tag{2.9}$$

With this decomposition, it must be noted that $\langle \psi_\beta \rangle^\beta$ has a typical length scale of variation L (see figure 1), while $\tilde{\psi}_\beta$ varies at the scale ℓ_β . The upscaling is subject to the scale hierarchy defined by $\ell_\beta \ll r_0 \ll L$, which can be used to prove that $\langle \langle \psi_\beta \rangle^\beta \rangle^\beta = \langle \psi_\beta \rangle^\beta$ and consequently that $\langle \tilde{\psi}_\beta \rangle^\beta = 0$ (Whitaker 1999). When the procedure is applied to the initial boundary value problem in (2.1), the following averaged mass, momentum and state equations are obtained (Lasseux *et al.* 2014)

$$\frac{\partial \langle \rho_\beta \rangle^\beta}{\partial t} + \nabla \cdot (\langle \rho_\beta \rangle^\beta \langle \mathbf{v}_\beta \rangle^\beta) = 0 \tag{2.10}$$

$$0 = -\nabla \langle p_\beta \rangle^\beta + \mu_\beta \nabla^2 \langle \mathbf{v}_\beta \rangle^\beta + \frac{1}{V_\beta} \int_{\mathcal{A}_{\beta\sigma}} \mathbf{n} \cdot (-\tilde{\mathcal{I}}\tilde{p}_\beta + \mu_\beta \nabla \tilde{\mathbf{v}}_\beta) dA \tag{2.11}$$

$$\langle \rho_\beta \rangle^\beta = F(\langle p_\beta \rangle^\beta). \tag{2.12}$$

To arrive at this form, the assumption of a slightly compressible flow, that is expressed through the constraint

$$\tilde{\rho}_\beta \ll \langle \rho_\beta \rangle^\beta \tag{2.13}$$

was employed, along with the homogeneity of the medium that allows the treating of ε as a constant.

The macroscale momentum equation (2.11) is not closed as it involves pressure and velocity deviations that are essentially varying at the pore scale. Therefore, one needs to derive and solve the associated closure problem that is written in terms of \tilde{p}_β and $\tilde{\mathbf{v}}_\beta$ over a periodic unit cell representative of the macroscopic region as (Lasseux *et al.* 2014)

$$\nabla \cdot \tilde{\mathbf{v}}_\beta = 0 \quad \text{in } \mathcal{V}_\beta \tag{2.14a}$$

$$0 = -\nabla \tilde{p}_\beta + \mu_\beta \nabla^2 \tilde{\mathbf{v}}_\beta - \frac{1}{V_\beta} \int_{\mathcal{A}_{\beta\sigma}} \mathbf{n} \cdot (-\tilde{\mathcal{I}}\tilde{p}_\beta + \mu_\beta \nabla \tilde{\mathbf{v}}_\beta) dA \quad \text{in } \mathcal{V}_\beta \tag{2.14b}$$

$$\tilde{\mathbf{v}}_\beta + \xi \bar{\lambda}_\beta (\mathbf{I} - \mathbf{nn}) \cdot (\mathbf{n} \cdot (\nabla \tilde{\mathbf{v}}_\beta + \nabla \tilde{\mathbf{v}}_\beta^T)) = -\langle \mathbf{v}_\beta \rangle^\beta \quad \text{at } \mathcal{A}_{\beta\sigma} \tag{2.14c}$$

$$\langle \tilde{p}_\beta \rangle^\beta = 0 \tag{2.14d}$$

$$\left. \begin{aligned} \text{Periodicity } \tilde{\mathbf{v}}_\beta(\mathbf{r} + \mathbf{l}_i) &= \tilde{\mathbf{v}}_\beta(\mathbf{r}), \\ \tilde{p}_\beta(\mathbf{r} + \mathbf{l}_i) &= \tilde{p}_\beta(\mathbf{r}), \quad i = 1, 2, 3. \end{aligned} \right\} \tag{2.14e}$$

This problem simply results from the subtraction of the averaged equations from their initial counterparts expressed in (2.1). In (2.14c), $\bar{\lambda}_\beta$ represents the mean free path at the average density, which defines the macroscale Knudsen number, $\bar{Kn} = \bar{\lambda}_\beta / \ell_\beta$ that will be used throughout this work. This definition of the Knudsen number is the most physically relevant as it reflects the wall effect occurring in the Knudsen layer (of thickness approximately given by the mean free path) relative to the size of the channel where the flow is taking place. Upon assuming molecular collisions between

hard spheres and considering the slightly compressible hypothesis, $\bar{\lambda}_\beta$ can be expressed as (Cowling 1950)

$$\bar{\lambda}_\beta = \frac{M}{\sqrt{2}\pi\mathcal{N}_A\langle\rho_\beta\rangle^\beta\delta^2}. \tag{2.15}$$

Here, \mathcal{N}_A is Avogadro’s number, M the molar mass of the gas and δ the gas particle diameter, $\pi\delta^2$ being the effective collision section.

While (2.14d) is necessary to define a well-posed problem, the analogue for the velocity deviation $\langle\tilde{\mathbf{v}}_\beta\rangle^\beta = 0$ is not, although this last relationship will be employed later. Equations (2.14) are subject to the slightly compressible flow hypothesis expressed in (2.13) and to the constraint of scale hierarchy $\ell_\beta \ll L$ similar to that employed in homogenization (Skjetne & Auriault 1999).

At this point, a closure procedure relating deviations to average quantities in the boundary value problem (2.14) is required in order to derive a closed macroscopic model. This is carried out in the next section, where a Darcy-like average momentum equation is obtained in which the apparent slip-corrected permeability, \mathbf{K}_s , is determined from the associated closure problem.

3. Closure and macroscopic model

A procedure to close the averaged momentum equation (2.11) from the deviation equations (2.14) was proposed and validated earlier, yielding a macroscopic model at $\mathcal{O}(\xi\bar{K}n)$, which involves the intrinsic permeability tensor \mathbf{K} and a slip-flow correction tensor \mathbf{S} (Lasseux *et al.* 2014). Both tensors are obtained from the solution of intrinsic closure problems that are coupled through a ‘slip-like’ boundary condition. Whereas the closure problem for \mathbf{K} can be written in a ‘Stokes-like’ form, \mathbf{S} derived from an integro-differential closure. In terms of solution strategy and physical interpretation, this represents a real difficulty that is removed in the development presented below.

3.1. Closure problem

A convenient closure is now derived by noticing that the boundary value problem for the deviations (2.14) at the pore scale is made non-homogeneous due to the macroscopic source term $\langle\mathbf{v}_\beta\rangle^\beta$ on the right-hand side of the boundary condition (2.14c). Since this problem is incompressible in nature, $\bar{\lambda}_\beta$ can be regarded as a parameter and does not represent a source for \tilde{p}_β and $\tilde{\mathbf{v}}_\beta$ despite its dependence on $\langle\rho_\beta\rangle^\beta$. Due to the linearity of the problem, the solution can be sought as a linear combination of the source, namely

$$\tilde{\mathbf{v}}_\beta = \mathbf{C} \cdot \langle\mathbf{v}_\beta\rangle^\beta \tag{3.1}$$

$$\tilde{p}_\beta = \mu_\beta \mathbf{c} \cdot \langle\mathbf{v}_\beta\rangle^\beta. \tag{3.2}$$

Any additive constant in the representations of $\tilde{\mathbf{v}}_\beta$ and \tilde{p}_β can be shown to be unimportant in the final macroscopic model, just as for the upscaling of the classical incompressible Stokes flow with no slip (Whitaker 1999). Using these representations in the closure equations (2.14), while treating $\langle\mathbf{v}_\beta\rangle^\beta$ as a constant due to the contrast of scale between ℓ_β and L , yields the following closure problem in terms of the closure variables \mathbf{C} and \mathbf{c}

$$\nabla \cdot \mathbf{C} = 0 \quad \text{in } \mathcal{V}_\beta \tag{3.3a}$$

$$0 = -\nabla \mathbf{c} + \nabla^2 \mathbf{C} - \frac{1}{V_\beta} \int_{\mathcal{A}_{\beta\sigma}} \mathbf{n} \cdot (-\mathbf{l}\mathbf{c} + \nabla \mathbf{C}) \, dA \quad \text{in } \mathcal{V}_\beta \tag{3.3b}$$

$$\mathbf{C} + \xi \bar{\lambda}_\beta (\mathbf{I} - \mathbf{nn}) \cdot (\mathbf{n} \cdot (\nabla \mathbf{C} + (\nabla \mathbf{C})^{T1})) = -\mathbf{l} \quad \text{at } \mathcal{A}_{\beta\sigma} \tag{3.3c}$$

$$\langle \mathbf{c} \rangle^\beta = 0 \tag{3.3d}$$

$$\left. \begin{aligned} \text{Periodicity } \mathbf{C}(\mathbf{r} + \mathbf{l}_i) &= \mathbf{C}(\mathbf{r}), \\ \mathbf{c}(\mathbf{r} + \mathbf{l}_i) &= \mathbf{c}(\mathbf{r}), \quad i = 1, 2, 3. \end{aligned} \right\} \tag{3.3e}$$

In (3.3c), the superscript $T1$ designates the transpose of a third-order tensor that permutes the two first indices (in Lasseux *et al.* 2014, equation (83c), we simply used the superscript T for this transpose and this was ambiguous). Note that (3.3d) follows from (2.14d) along with the pressure representation in (3.2) and is required for (3.3) to form a well-posed problem.

At this point, a simple transformation, similar to that employed while upscaling the incompressible creeping flow with no slip leading to Darcy’s law, can be used to obtain a pure differential form of this closure (Barrère, Gipouloux & Whitaker 1992; Whitaker 1999). Letting

$$\mathbf{K}_s^{-1} = -\varepsilon^{-1} \frac{1}{V_\beta} \int_{\mathcal{A}_{\beta\sigma}} \mathbf{n} \cdot (-\mathbf{l}\mathbf{c} + \nabla \mathbf{C}) \, dA \tag{3.4}$$

defining \mathbf{D} and \mathbf{d} as

$$\mathbf{D} = \varepsilon^{-1} (\mathbf{C} + \mathbf{l}) \cdot \mathbf{K}_s \tag{3.5}$$

$$\mathbf{d} = \varepsilon^{-1} \mathbf{c} \cdot \mathbf{K}_s \tag{3.6}$$

and returning to (3.3) yields the following local closure problem

$$\nabla \cdot \mathbf{D} = 0 \quad \text{in } \mathcal{V}_\beta \tag{3.7a}$$

$$0 = -\nabla \mathbf{d} + \nabla^2 \mathbf{D} + \mathbf{l} \quad \text{in } \mathcal{V}_\beta \tag{3.7b}$$

$$\mathbf{D} = -\xi \bar{\lambda}_\beta (\mathbf{I} - \mathbf{nn}) \cdot (\mathbf{n} \cdot (\nabla \mathbf{D} + (\nabla \mathbf{D})^{T1})) \quad \text{at } \mathcal{A}_{\beta\sigma} \tag{3.7c}$$

$$\langle \mathbf{d} \rangle^\beta = 0 \tag{3.7d}$$

$$\langle \mathbf{D} \rangle = \mathbf{K}_s \tag{3.7e}$$

$$\left. \begin{aligned} \text{Periodicity } \mathbf{D}(\mathbf{r} + \mathbf{l}_i) &= \mathbf{D}(\mathbf{r}), \\ \mathbf{d}(\mathbf{r} + \mathbf{l}_i) &= \mathbf{d}(\mathbf{r}), \quad i = 1, 2, 3. \end{aligned} \right\} \tag{3.7f}$$

From this tractable form having the structure of an incompressible Stokes problem with a slip boundary condition, \mathbf{K}_s can be computed from a simple average on \mathbf{D} as indicated in (3.7e). This last equation is not required in the solution procedure but is used as a direct consequence of the definition of \mathbf{D} in (3.5) together with the intrinsic average of the velocity decomposition in (3.1), which yields $\langle \mathbf{C} \rangle^\beta = 0$. Although local, the closure (3.7) is non-intrinsic due to the presence of $\xi \bar{\lambda}_\beta$ in the boundary condition of (3.7c) and we shall come back to this in §4.

3.2. Closed macroscopic model

When the representation of the deviations given in (3.1) and (3.2) are reported in the unclosed form of the averaged momentum equation (2.11), one readily obtains a Darcy-like macroscopic law

$$0 = -\nabla \langle p_\beta \rangle^\beta - \mu_\beta \mathbf{K}_s^{-1} \cdot \langle \mathbf{v}_\beta \rangle + \mu_\beta \varepsilon^{-1} \nabla^2 \langle \mathbf{v}_\beta \rangle, \tag{3.8}$$

which, along with (2.10) and (2.12), forms the closed averaged model for the slightly compressible slip flow considered in this work. In (3.8), \mathbf{K}_s , defined in (3.7e), is identified as the apparent slip-corrected permeability.

The last term on the right-hand side of (3.8) is referred to as the Brinkman correction. An order of magnitude analysis can be used to show that this macroscale viscous diffusion term has a negligible contribution in the bulk of the porous medium. Indeed, as can be inferred from the boundary condition in (2.14c)

$$\tilde{\mathbf{v}}_\beta = \mathbf{O} \left(\frac{\langle v_\beta \rangle^\beta}{1 + \xi \overline{Kn}} \right), \tag{3.9}$$

where $\langle v_\beta \rangle^\beta$ represents the leading order of $\langle \mathbf{v}_\beta \rangle^\beta$. This shows that

$$\mathbf{C} = \mathbf{O}((1 + \xi \overline{Kn})^{-1}) \tag{3.10}$$

and consequently, from the definition of \mathbf{K}_s in (3.4), the order of magnitude of the Darcy term in (3.8) can be estimated as

$$\mu_\beta \mathbf{K}_s^{-1} \cdot \langle \mathbf{v}_\beta \rangle = \mathbf{O}(\mu_\beta \varepsilon^{-2} \ell_\beta^{-1} (1 + \xi \overline{Kn})^{-1} a_v \langle v_\beta \rangle^\beta). \tag{3.11}$$

In this estimate, $a_v = A_{\beta\sigma}/V$ represents the interfacial area per unit volume of the medium that is expected to scale as ℓ_β^{-1} . Similarly, the order of magnitude of the Brinkman term can be estimated to be

$$\mu_\beta \varepsilon^{-1} \nabla^2 \langle \mathbf{v}_\beta \rangle = \mathbf{O}(\mu_\beta L^{-2} \langle v_\beta \rangle^\beta), \tag{3.12}$$

which, when compared to (3.11), clearly indicates that the Brinkman term is completely negligible in the context of slip flow, i.e. when $\xi \overline{Kn} \lesssim 0.1$. The macroscopic model can hence be written, to within an approximation $\mathbf{O}(\ell_\beta/L)$, as

$$\frac{\partial \langle \rho_\beta \rangle^\beta}{\partial t} + \nabla \cdot (\langle \rho_\beta \rangle^\beta \langle \mathbf{v}_\beta \rangle^\beta) = 0 \tag{3.13a}$$

$$0 = -\nabla \langle p_\beta \rangle^\beta - \mu_\beta \mathbf{K}_s^{-1} \cdot \langle \mathbf{v}_\beta \rangle \tag{3.13b}$$

$$\langle \rho_\beta \rangle^\beta = F(\langle p_\beta \rangle^\beta). \tag{3.13c}$$

It must be noted that the apparent slip-corrected permeability, \mathbf{K}_s , in the Darcy-like form of the macroscopic momentum equation (3.13b) is non-intrinsic as it lumps together topological properties, intrinsic to the microstructure of the medium, and slip effects that depend on the slip length $\xi \bar{\lambda}_\beta$. Moreover, a detailed analysis, provided in appendix A, indicates that, unlike the intrinsic permeability that is the fundamental coefficient in the classical Darcy’s law when no slip occurs, \mathbf{K}_s is not symmetric in the general case. Quasi-symmetry is observed under the constraint

$$\xi \overline{Kn} \ll \mathbf{O}(\varepsilon) \tag{3.14}$$

that is also detailed and illustrated in appendix A, completing a previous analysis of this property (Skjetne & Auriault 1999). An important consequence is that the full characterization of the tensor \mathbf{K}_s from a measurement point of view is significantly simplified when the constraint in (3.14) is satisfied.

In § 3.3 below, the validity of the macroscopic model and of the associated closure problem (3.7) yielding \mathbf{K}_s is verified by comparison with analytic solutions in a simple configuration and with direct numerical simulations on a more complex medium.

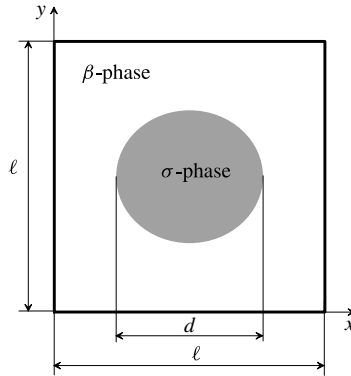


FIGURE 2. Unit cell for the square lattice of cylinders of circular cross-section.

3.3. Validation

The finite element solver Comsol Multiphysics 4.4 was used to carry out the numerical solutions of both the pore-scale equations (2.1) and the closure problem (3.7). Meshing tests were carried out to reach convergence and led to the use of nearly 13 000 domain mesh elements with more than 500 boundary elements. This mesh was built by adding a boundary layer at the solid–fluid interface with a stretching factor of 1.2. As a first validation, a simple structure made of a periodic square pattern of parallel circular cylinders was considered, as represented in figure 2.

The slip flow orthogonal to the cylinder axes is such that $\mathbf{K}_s = k_s \mathbf{I}$, where k_s can be computed from the solution of the projection of the closure problem either on \mathbf{e}_x or \mathbf{e}_y . Due to the unit cell symmetry, the projection leads to a boundary value problem equivalent to the initial incompressible pore-scale problem when symmetry on the velocity and Dirichlet boundary conditions on the pressure are applied on faces respectively parallel and orthogonal to the mean flow direction. Taking the projection of the closure problem (3.7) on \mathbf{e}_x , the equivalence is obvious when $\mathbf{D} \cdot \mathbf{e}_x$ and $\mathbf{d} \cdot \mathbf{e}_x$ are respectively identified as $\mu \mathbf{v}_\beta / \|\nabla \langle p_\beta \rangle^\beta\|$ and $\tilde{p}_\beta / \|\nabla \langle p_\beta \rangle^\beta\|$ in the incompressible version of the pore-scale flow problem (2.1). The validation of the macroscopic model through a comparison of k_s obtained either from the closure problem solution or from a DNS of the initial boundary value problem is hence trivial in that case. Nevertheless, further validation can be made by comparing numerical results on k_s with analytic predictions obtained on a Chang’s unit cell (Chai *et al.* 2011; Lasseux *et al.* 2014) which has been shown to be a reliable estimate for the periodic structure under consideration.

The closure problem was solved on the unit cell of figure 2 for $\varepsilon = 0.8$. Examples of the dimensionless xx component of \mathbf{D} and x component of \mathbf{d} are reported in figure 3 for two values of the cell Knudsen number $\xi \bar{\lambda}_\beta^* = \xi \bar{\lambda}_\beta / \ell$. Note that $\xi \bar{\lambda}_\beta^* = \xi \bar{K} n \ell_\beta^* = \xi \bar{K} n \ell_\beta / \ell$. The closure fields represented in figures 3(a) and 3(b) are, in fact, the x components of the velocity field made dimensionless by $\ell^2 \|\nabla \langle p_\beta \rangle^\beta\| / \mu_\beta$ whereas the closure fields in figures 3(c) and 3(d) are the pressure deviation fields made dimensionless by $\ell \|\nabla \langle p_\beta \rangle^\beta\|$.

Numerical results on $k_s^* = k_s / \ell^2$ are reported in figure 4a versus $\xi \bar{\lambda}_\beta^* = \xi \bar{\lambda}_\beta / \ell$, for $\varepsilon = 0.8$. As discussed elsewhere (Lasseux *et al.* 2014), a Chang’s unit cell, composed of the solid cylinder immersed in a circular fluid shell, may be used, along with a

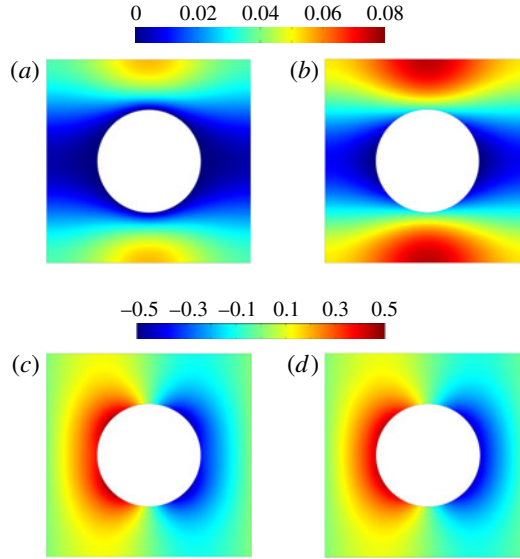


FIGURE 3. (Colour online) Dimensionless closure variable fields computed on the unit cell of figure 2, $\varepsilon = 0.8$: (a) D_{xx}/ℓ^2 , $\xi\bar{\lambda}_\beta^* = 10^{-4}$; (b) D_{xx}/ℓ^2 , $\xi\bar{\lambda}_\beta^* = 0.1$; (c) d_x/ℓ , $\xi\bar{\lambda}_\beta^* = 10^{-4}$; (d) d_x/ℓ , $\xi\bar{\lambda}_\beta^* = 0.1$.

zero vorticity boundary condition at the outer edge, to derive an approximate analytic solution. For this relatively large value of the porosity, it is given by

$$k_s^* = \frac{1}{8\pi \left(1 + 2\xi\bar{\lambda}_\beta^* \sqrt{\frac{\pi}{\phi}}\right)} \left(-\ln \phi - \frac{3}{2} + 2\phi - \frac{\phi^2}{2} + 2\xi\bar{\lambda}_\beta^* \sqrt{\frac{\pi}{\phi}} \left(-\ln \phi - \frac{1}{2} + \frac{\phi^2}{2} \right) \right), \quad (3.15)$$

where $\phi = 1 - \varepsilon$.

The agreement of the prediction from (3.15) with our numerical results is excellent, as shown in figure 4. The relative error on k_s^* , taking the computed value as the reference, is less than 0.4% over the interval $10^{-4} \leq \xi\bar{\lambda}_\beta^* \leq 0.13$. Within this range of $\xi\bar{\lambda}_\beta^*$, $\xi\bar{Kn}$ remains smaller than ~ 0.23 when $\ell_\beta^* = \ell_\beta/\ell$ is estimated from the slit aperture of the equivalent bundle of regularly spaced parallel plates given by $\ell_\beta^* = 2\sqrt{3k^*/\varepsilon}$, $k^* = k/\ell^2$ being the dimensionless intrinsic permeability, i.e. the permeability without slip. As clearly indicated in figure 4b, representing k_s^*/k^* versus $\xi\bar{Kn}$, k_s^* exhibits a nonlinear dependence on the Knudsen number even though the flow is expected to remain in the slip regime at the microscale. This important remark will be analysed in more detail in §4.2.

An additional validation is now investigated in the case of a more complex 2-D structure featuring no special symmetry properties and for which no analytic solution is available. In that case, validation of both the upscaling procedure and macroscopic model can be achieved through the comparison of DNS of the pore-scale flow problem (2.1) with the numerical solution of the closure problem (3.7).

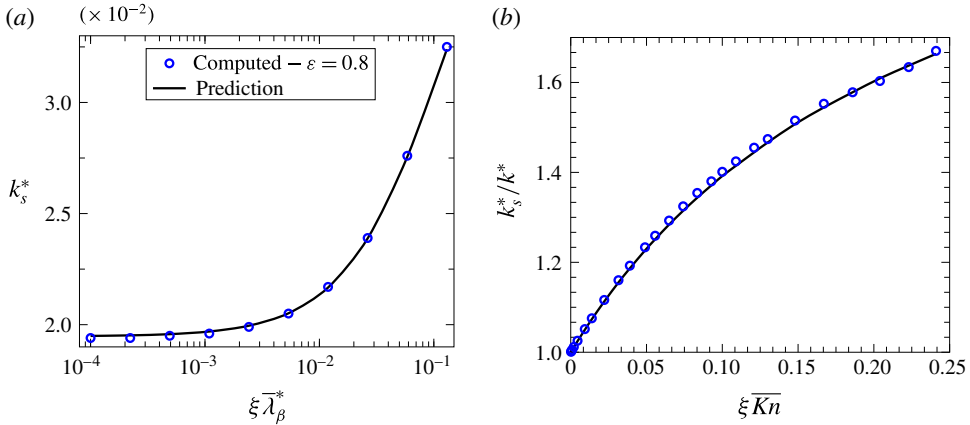


FIGURE 4. (Colour online) Dimensionless apparent slip-corrected permeability $k_s^* = k_s/\ell^2$ for the unit cell of figure 2, $\varepsilon = 0.8$, $k^* = k/\ell^2 \simeq 0.01938$, k being the intrinsic permeability: (a) k_s^* versus $\xi \bar{\lambda}_\beta^* = \xi \bar{\lambda}_\beta/\ell$, comparison between the computed values obtained from the solution of the closure problem (3.7) and the analytic prediction from (3.15); (b) k_s^*/k^* versus $\xi \bar{Kn} = \xi \bar{\lambda}_\beta^*/\ell_\beta^*$, ℓ_β^* being the dimensionless distance between parallel plates that would exhibit the same intrinsic permeability, i.e. $\ell_\beta^* = 2\sqrt{3k^*/\varepsilon}$.

The structure at scale L for DNS is obtained by duplicating n times, in the direction of the applied macroscopic pressure gradient, a periodic unit cell of size ℓ made of randomly placed cylinders of circular cross-sections with randomly chosen radii within a prescribed interval $[r_{min}, r_{max}]$ according to a log-normal distribution. Placement of cylinder centres is constrained to ensure periodicity in the x and y directions and is repeated until a target porosity is achieved, while controlling cylinders overlapping.

Two random unit cells, of porosity $\varepsilon = 0.375$ and $\varepsilon = 0.804$, were generated using respectively $r_{min} = 0.023\ell$, $r_{max} = 0.062\ell$ and $r_{min} = 0.016\ell$, $r_{max} = 0.031\ell$. They were used to compute the xx dimensionless component, $k_{sxx}^* = k_{sxx}/\ell^2$, of the apparent slip-corrected permeability tensor from the closure problem solution. In addition, DNS were performed on structures at scale L obtained from these generic unit cells with n , the number of unit cell replicas, ranging from 3 to 9. Constant pressures were prescribed at the entrance ($x = 0$) and exit ($x = L$) of the structure while periodic boundary conditions were applied in the y direction. Superficial and intrinsic averages of $\mathbf{v}_\beta \cdot \mathbf{e}_x$ and p_β were performed on the central unit cell $(n + 1)/2$ to compute k_{sxx}^* . Computations were carried out for $10^{-4} \leq \xi \bar{\lambda}_\beta^* \leq 10^{-2}$.

The DNS procedure is illustrated in figure 5 where we have represented an example of the two L -scale structures, along with the two generic unit cells on which maps of $\mathbf{v}_\beta \cdot \mathbf{e}_x$ were superimposed. In this figure, we have also reported the pressure profiles computed on the left vertical edge of the central unit cell. The evident non-uniformity of p_β explains why DNS cannot be carried out on a single unit cell with predefined entrance/exit constant Dirichlet boundary conditions on the pressure.

As shown in table 1 and in figure 6a, results on k_{sxx}^* obtained from DNS and the closure problem solution are in excellent agreement since the relative error is less than 1.3% and decreases when n increases, confirming the validity of the macroscopic model and associated closure.

In figure 6b, a clear nonlinear dependence of k_{sxx}^* on $\xi \bar{Kn}$, most pronounced for the largest value of the porosity, is again highlighted for the two unit cells of figure 5b,

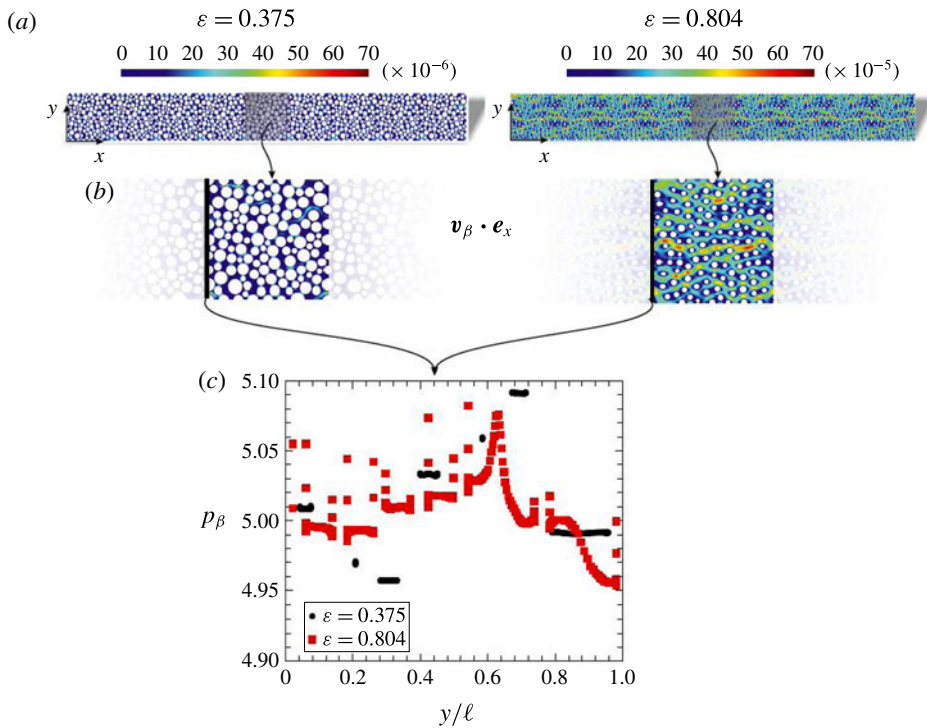


FIGURE 5. (Colour online) Slip-flow DNS on 2-D packs of cylinders. (a) Large-scale structures obtained from periodic replicas along e_x of random unit cells. Velocity maps in the x direction are superimposed. (b) Random unit cells of respective porosity $\varepsilon = 0.375$ and $\varepsilon = 0.804$ used to generate large-scale structures along with x -velocity maps. (c) Pressure profiles at the left edge of the central unit cells.

n	$\xi \bar{\lambda}_\beta^* = 10^{-4}$				$\xi \bar{\lambda}_\beta^* = 10^{-2}$			
	$\varepsilon = 0.375$		$\varepsilon = 0.804$		$\varepsilon = 0.375$		$\varepsilon = 0.804$	
	$k_{sxx}^* \times 10^{-6}$	Error %	$k_{sxx}^* \times 10^{-4}$	Error %	$k_{sxx}^* \times 10^{-5}$	Error %	$k_{sxx}^* \times 10^{-4}$	Error %
3	2.711	1.25	1.647	0.56	1.043	1.07	2.542	0.54
5	2.695	0.62	1.642	0.29	1.035	0.33	2.536	0.32
7	2.685	0.26	1.640	0.17	1.028	0.40	2.535	0.27
9	2.678	0.02	1.639	0.06	1.029	0.24	2.534	0.25

TABLE 1. Comparison of the predictions of k_{sxx}^* from DNS with those from volume averaging. n is the number of unit cell replicas. k_{sxx}^* values are those obtained from DNS taking the average at the $(n + 1)/2$ unit cell. The error per cent is computed relative to the DNS predictions.

although $\xi \bar{Kn}$ remains smaller than approximately 0.23, a range typical of the slip-flow regime as justified by some measurements for even larger Knudsen numbers in straight channels (Harley *et al.* 1995). This confirms the behaviour reported above for the regular square pattern of cylinders.

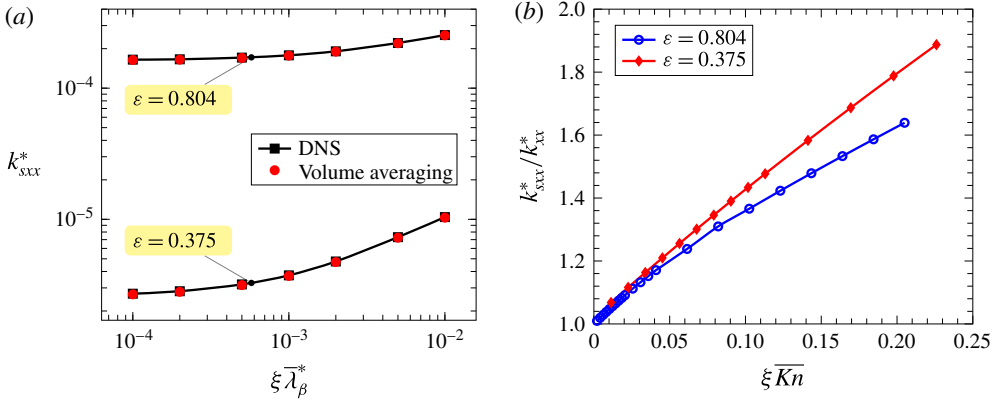


FIGURE 6. (Colour online) (a) Comparison of computed values of k_{sxx}^* obtained from DNS and volume averaging for the two unit cells of figure 5(b). (b) Dependence of k_{sxx}^*/k_{xx}^* on $\xi \bar{Kn} = \xi \bar{\lambda}_\beta^* \ell / \ell_\beta = \xi \bar{\lambda}_\beta^* / \ell_\beta^*$ for $\xi \bar{Kn} \lesssim 0.2$. Here $\xi \bar{Kn}$ is estimated from the dimensionless distance between plane parallel plates, $\ell_\beta^* = 2\sqrt{3k^*/\varepsilon}$, that would lead to the same intrinsic permeability $k^* = k_{xx}^*$. $k_{xx}^* \simeq 2.44 \times 10^{-6}$ ($\varepsilon = 0.375$); $k_{xx}^* \simeq 1.60 \times 10^{-4}$ ($\varepsilon = 0.804$).

At this point it is worth mentioning that, in the seminal work of Klinkenberg (1941), the linear dependence of the apparent permeability with the Knudsen number was regarded as an approximation resulting from a representation of the porous medium as a system of straight capillaries. As a matter of fact, Klinkenberg (1941) noticed some nonlinearities in his experimental results with the same tendency as the one observed here. However, the porous media that he considered were relatively tight with intrinsic permeabilities that could go as low as 2.4 mDarcy. As a consequence, the porosity is expected to be quite small and this may explain why the observed nonlinearity remained not too drastic in his experimental results. As shown in figure 6(b), our predictions indicate that the nonlinearity decreases as porosity decreases and becomes almost insignificant for a porosity of 0.25, which is in a qualitative agreement with Klinkenberg’s results.

Before considering in more detail the above mentioned nonlinearity, the impact of an incomplete version of the slip boundary condition, in which the $\nabla \mathbf{v}_\beta^T$ term is omitted, shall be illustrated. When such an incomplete boundary condition is employed, the analytic form of the apparent slip-corrected permeability of the periodic square pattern of parallel circular cylinders, for a sufficiently large porosity ($\varepsilon \gtrsim 0.55$), is given by

$$\begin{aligned}
 k_s^* = & \frac{1}{8\pi \left(1 + 2\xi \bar{\lambda}_\beta^* \sqrt{\frac{\pi}{\phi}}\right)} \left(-\ln \phi - \frac{3}{2} + 2\phi - \frac{\phi^2}{2} \right. \\
 & \left. + \xi \bar{\lambda}_\beta^* \sqrt{\frac{\pi}{\phi}} \left(-\ln \phi + \frac{1}{2} - 2\phi + \frac{3\phi^2}{2} \right) \right) \quad (3.16)
 \end{aligned}$$

instead of (3.15) above, with again $\phi = 1 - \varepsilon$. This last expression underestimates k_s^* obtained from (3.15). The two slip-flow corrections can be extracted from (3.15) and (3.16) as $k_s^*/k^* - 1$, where $k^* = 1/8\pi(-\ln \phi - (3/2) + 2\phi - \phi^2/2)$ is again the dimensionless intrinsic permeability and the relative error between the two, taking the

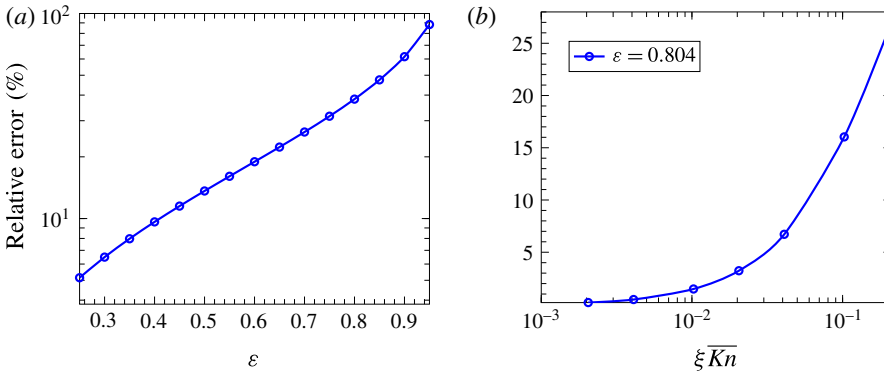


FIGURE 7. (Colour online) Relative error on the slip correction while using an incomplete slip boundary condition (i.e. omitting the $\nabla \mathbf{v}_\beta^T$ term). (a) Unit cell of figure 2. The error is computed from the analytic expressions (3.15) and (3.16). (b) Random pack of parallel cylinders (see figure 5b), $\varepsilon = 0.804$. The error is computed from the closure problem solutions using complete and incomplete boundary conditions at $\mathcal{A}_{\beta\sigma}$.

former as the reference, is given by $(-2 \ln \phi - 3 + 4\phi - \phi^2)/(4(1 - 2\phi + \phi^2))$. This relative % error, independent of $\xi\bar{Kn}$, is represented versus the porosity in figure 7a showing an increasingly significant error with ε , as it can reach approximately 62 % for $\varepsilon = 0.9$.

When the $\nabla \mathbf{v}_\beta^T$ term is omitted in the pore-scale slip boundary condition, the closure problem (3.7) is unchanged, except the term $(\nabla \mathbf{D})^{T1}$ that is no longer present in (3.7c). This form of the closure was solved on the unit cell of the random pack of parallel cylinders (see figure 5b) for $\varepsilon = 0.804$, yielding k_{xxx}^* that turns out to be larger than that obtained with the complete boundary condition. The slip correction can again be estimated from $k_{xxx}^*/k^* - 1$ computed with and without the complete shear rate in the boundary condition and the relative error can be formed taking the former as the reference. This % error, represented versus $\xi\bar{Kn}$ in figure 7b, remains small at exceedingly small values of the Knudsen number (approximately 7 % for $\xi\bar{Kn} \simeq 0.04$), but strongly increases with $\xi\bar{Kn}$ as it reaches approximately 26 % for $\xi\bar{Kn} \simeq 0.2$. This clearly evidences that the complete strain rate must be kept in the expression of the slip at the solid boundary. More insight on the impact of the form of the boundary condition and on the nonlinear behaviour mentioned above will be provided in §4, following a reformulation of the closure problem.

4. Reformulation and effective intrinsic coefficients

In the macroscopic model developed above, both viscous and slip effects are lumped together in the apparent slip-corrected permeability \mathbf{K}_s that is determined by a non-intrinsic closure problem. To isolate the Knudsen contribution to the flow at the macroscopic scale and to identify intrinsic macroscopic coefficients, the closure problem in (3.7) needs to be further developed.

4.1. Expansion in $\xi\bar{Kn}$

The development is carried out on the dimensionless form of the closure given by the starred dimensionless quantities $\mathbf{d}^* = \mathbf{d}/\ell_\beta$, $\mathbf{D}^* = \mathbf{D}/\ell_\beta^2$, $\nabla^* = \ell_\beta \nabla$ as

$$\nabla^* \cdot \mathbf{D}^* = 0 \quad \text{in } \mathcal{V}_\beta \tag{4.1a}$$

$$0 = -\nabla^* \mathbf{d}^* + \nabla^{*2} \mathbf{D}^* + \mathbf{I} \quad \text{in } \mathcal{V}_\beta \tag{4.1b}$$

$$\mathbf{D}^* = -\xi \overline{Kn} (\mathbf{I} - \mathbf{nn}) \cdot (\mathbf{n} \cdot (\nabla^* \mathbf{D}^* + (\nabla^* \mathbf{D}^*)^{T1})) \quad \text{at } \mathcal{A}_{\beta\sigma} \tag{4.1c}$$

$$\langle \mathbf{d}^* \rangle^\beta = 0 \tag{4.1d}$$

$$\langle \mathbf{D}^* \rangle = \mathbf{K}_s \ell_\beta^{-2} \tag{4.1e}$$

$$\left. \begin{aligned} \text{Periodicity } \mathbf{D}^*(\mathbf{r}^* + \mathbf{l}_i^*) &= \mathbf{D}^*(\mathbf{r}^*), \\ \mathbf{d}^*(\mathbf{r}^* + \mathbf{l}_i^*) &= \mathbf{d}^*(\mathbf{r}^*), \quad i = 1, 2, 3. \end{aligned} \right\} \tag{4.1f}$$

Since $\xi \overline{Kn}$ remains smaller than unity in the context of slip flow, \mathbf{d}^* and \mathbf{D}^* can be developed up to the m th order in Maclaurin series expansions that we shall write as

$$\mathbf{d}^* = \mathbf{d}_0^* + \sum_{j=1}^m (\xi \overline{Kn})^j \mathbf{e}_j^* + R_{dm} \tag{4.2}$$

and

$$\mathbf{D}^* = \mathbf{D}_0^* + \sum_{j=1}^m (\xi \overline{Kn})^j \mathbf{E}_j^* + R_{Dm}, \tag{4.3}$$

where R_{dm} and R_{Dm} are the residuals at the m th order. When these expansions are introduced back into (4.1), the closure problem can be split in a series of closures that ensue from the identification at the successive orders in $\xi \overline{Kn}$. Returning to the dimensional form, the closure problem at the 0th order takes the form

0th order:

$$\nabla \cdot \mathbf{D}_0 = 0 \quad \text{in } \mathcal{V}_\beta \tag{4.4a}$$

$$0 = -\nabla \mathbf{d}_0 + \nabla^2 \mathbf{D}_0 + \mathbf{I} \quad \text{in } \mathcal{V}_\beta \tag{4.4b}$$

$$\mathbf{D}_0 = 0 \quad \text{at } \mathcal{A}_{\beta\sigma} \tag{4.4c}$$

$$\langle \mathbf{d}_0 \rangle^\beta = 0 \tag{4.4d}$$

$$\left. \begin{aligned} \text{Periodicity } \mathbf{D}_0(\mathbf{r} + \mathbf{l}_i) &= \mathbf{D}_0(\mathbf{r}), \\ \mathbf{d}_0(\mathbf{r} + \mathbf{l}_i) &= \mathbf{d}_0(\mathbf{r}), \quad i = 1, 2, 3. \end{aligned} \right\} \tag{4.4e}$$

This closure problem exactly corresponds to that defining the intrinsic permeability, \mathbf{K} , while carrying out the upscaling of the incompressible Stokes problem without slip (Barrère *et al.* 1992; Whitaker 1999), and this means that

$$\langle \mathbf{D}_0 \rangle = \mathbf{K}. \tag{4.5}$$

Taking this relationship into account, along with the expansion of (4.3) and the definition of \mathbf{K}_s in (3.7e), allows writing, at the m th order

$$\mathbf{K}_s \simeq \mathbf{K} \cdot \left(\mathbf{I} + \sum_{j=1}^m (\xi \overline{\lambda}_\beta)^j \mathbf{S}_j \right). \tag{4.6}$$

Here \mathbf{S}_j ($j = 1, \dots, m$) is the macroscopic coefficient obtained from the closure problem at the j th order given, in its dimensional form, by

j th order ($j = 1, \dots, m$):

$$\nabla \cdot \mathbf{D}_j = 0 \quad \text{in } \mathcal{V}_\beta \tag{4.7a}$$

$$0 = -\nabla \mathbf{d}_j + \nabla^2 \mathbf{D}_j \quad \text{in } \mathcal{V}_\beta \tag{4.7b}$$

$$\mathbf{D}_j = -(\mathbf{I} - \mathbf{nn}) \cdot (\mathbf{n} \cdot (\nabla \mathbf{D}_{j-1} + (\nabla \mathbf{D}_{j-1})^{T1})) \quad \text{at } \mathcal{A}_{\beta\sigma} \tag{4.7c}$$

$$\langle \mathbf{d}_j \rangle^\beta = 0 \tag{4.7d}$$

$$\langle \mathbf{D}_j \rangle = \mathbf{K} \cdot \mathbf{S}_j \tag{4.7e}$$

$$\left. \begin{aligned} \text{Periodicity } \mathbf{D}_j(\mathbf{r} + \mathbf{l}_i) &= \mathbf{D}_j(\mathbf{r}), \\ \mathbf{d}_j(\mathbf{r} + \mathbf{l}_i) &= \mathbf{d}_j(\mathbf{r}), \quad i = 1, 2, 3. \end{aligned} \right\} \tag{4.7f}$$

In this j th-order problem, \mathbf{d}_j and \mathbf{D}_j represent the closure variables defined from their analogues, $\mathbf{e}_j = \ell_\beta \mathbf{e}_j^*$ and $\mathbf{E}_j = \ell_\beta^2 \mathbf{E}_j^*$ ($j = 1, \dots, m$), after applying the rescaling

$$\mathbf{d}_j = \mathbf{e}_j / (\ell_\beta)^j \tag{4.8}$$

$$\mathbf{D}_j = \mathbf{E}_j / (\ell_\beta)^j. \tag{4.9}$$

As a consequence, the macroscopic model at the m th order in $\xi \overline{Kn}$ takes the form

$$\varepsilon \frac{\partial \langle \rho_\beta \rangle^\beta}{\partial t} + \nabla \cdot (\langle \rho_\beta \rangle^\beta \langle \mathbf{v}_\beta \rangle) = 0 \tag{4.10a}$$

$$\langle \mathbf{v}_\beta \rangle \simeq -\frac{1}{\mu_\beta} \mathbf{K} \cdot \left(\mathbf{I} + \sum_{j=1}^m (\xi \overline{\lambda}_\beta)^j \mathbf{S}_j \right) \cdot \nabla \langle p_\beta \rangle^\beta \tag{4.10b}$$

$$\langle \rho_\beta \rangle^\beta = F(\langle p_\beta \rangle^\beta) \tag{4.10c}$$

in which $(\xi \overline{\lambda}_\beta)^j \mathbf{S}_j$ is the macroscopic j th-order slip-flow correction. The tensors \mathbf{K} and \mathbf{S}_j are respectively given by (4.5) and (4.7e) once the closure problems of (4.4) and (4.7) are solved. All these macroscopic coefficients are intrinsic as they derive from boundary value problems that only depend on the microstructure of the medium. At the first order, the macroscopic model is formally identical to that previously derived (Lasseux *et al.* 2014), and generalizes the classical Darcy–Klinkenberg form (Klinkenberg 1941) when the gas is ideal. However, it must be noted that the form of the first-order correction can be more complex than the dependence on $1/\langle p_\beta \rangle^\beta$ predicted by the classical Klinkenberg correction if a different state law is to be considered.

One must be clear that the expansion carried out in $\xi \overline{Kn}$ at the closure level is an alternative representation of the original closure problem given by (3.7) that is basically local, and this is quite a different approach from the one followed by Skjetne & Auriault (1999) that requires an additional constraint on the Knudsen number. The approach, in this last reference, potentially allows us to take into account non-local effects that could play a role while studying gas slip momentum transport near macroscopic boundaries.

Under the form of (4.10b), the macroscopic momentum equation clearly indicates that the apparent slip-corrected permeability, up to the first order, remains linear in $\xi \overline{Kn}$. As a consequence, the nonlinear behaviour observed in figures 4(b) and 6(b) can only be captured by higher-order terms in the macroscopic model, and this is a major result of the present development. In this perspective, a more thorough analysis of the macroscopic slip-flow correction, beyond the first order is proposed in §4.2.

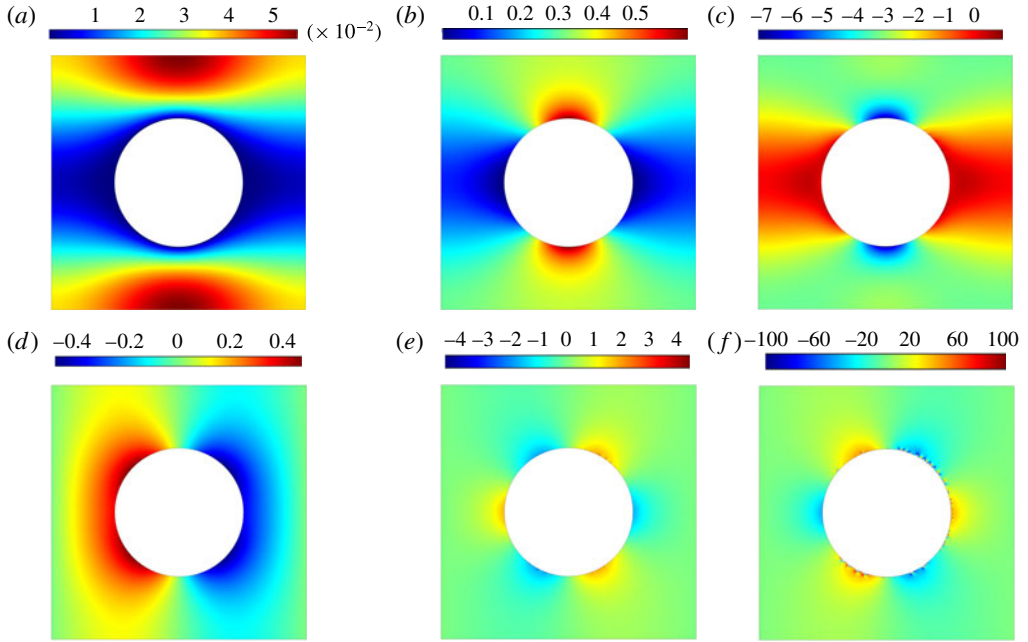


FIGURE 8. (Colour online) Dimensionless closure variable fields up to the second order computed on the unit cell of figure 2, $\varepsilon = 0.8$; (a) D_{0xx}/ℓ^2 ; (b) D_{1xx}/ℓ^2 ; (c) D_{2xx}/ℓ^2 ; (d) d_{0x}/ℓ ; (e) d_{1x}/ℓ ; (f) d_{2x}/ℓ .

4.2. Effective coefficients

All the closure problems providing the tensors \mathbf{K} and \mathbf{S}_j have an incompressible Stokes structure, the latter being coupled to each other and to the 0th-order problem through the slip-like boundary condition, which makes them non-homogeneous. Therefore, a unique numerical procedure can be used to determine all the macroscopic coefficients in a simple manner.

The same computational tool as the one employed for the determination of the apparent slip-corrected permeability, \mathbf{K}_s , (see §§ 3.1 and 3.3), was used to solve the closure problems (4.4) and (4.7) up to $m = 3$ on the model structure represented by the unit cell of figure 2 and ε ranging from 0.25 to 0.8. Due to the symmetries in this particular case, all the macroscopic coefficients are spherical tensors ($\mathbf{K} = k\mathbf{I}$, $\mathbf{S}_j = s_j\mathbf{I}$), thus requiring the solution of the projection of the corresponding closure problems on \mathbf{e}_x (or \mathbf{e}_y) only. Fields of the xx component of the tensors \mathbf{D}_0 , \mathbf{D}_1 , \mathbf{D}_2 and of the x components of the vectors \mathbf{d}_0 , \mathbf{d}_1 , \mathbf{d}_2 are reported in their dimensionless forms in figure 8.

In figure 9(a), we have represented $k^* = k/\ell^2$ versus ε , which shows an excellent agreement with our previous results (Lasseux *et al.* 2014) as well as with predictions available in the literature in the range of small (Bruschke & Advani 1993) and large (Kuwabara 1959) porosities.

Dimensionless slip-flow corrective terms, $k^*s_j^* = k^*(\ell)^j s_j$ are represented versus ε in figure 9b for $j = 1$ to 3. In this figure, we have also reported the $O(\xi\bar{K}n)$ slip-flow corrective term k^*s^* appearing in the classical macroscopic model as the one reported earlier (Lasseux *et al.* 2014). A perfect agreement with the first-order term of the present model can be observed, showing the equivalence of the two approaches

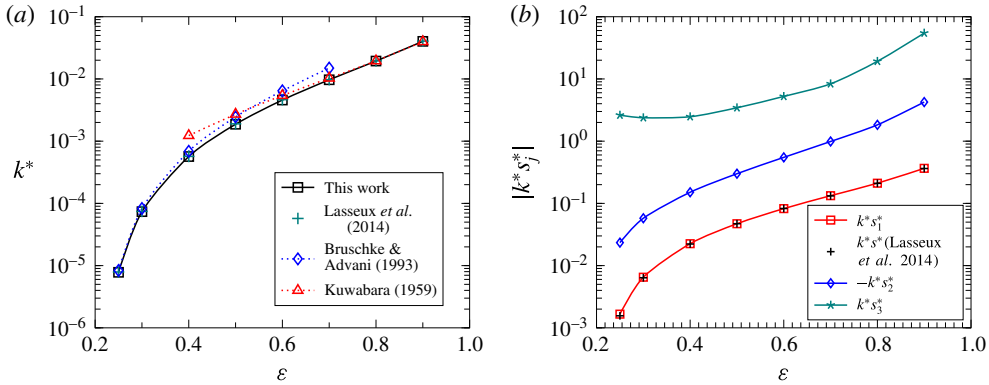


FIGURE 9. (Colour online) Dimensionless effective coefficients for slip flow versus ε . Unit cell of figure 2. (a) Intrinsic permeability. (b) Slip-flow corrective terms $k^* s_j^*$ for $j = 1-3$. Note that s_2^* is negative.

restricted to the first order in $\xi \bar{Kn}$. Higher-order terms in the present model are such that s_j is positive when j is odd and negative otherwise.

As can be inferred from the nonlinear dependence of k_s on the Knudsen number reported above, the first-order macroscopic slip correction might become relatively inaccurate in some circumstances. This is highlighted in figure 10 where we have reported the apparent slip-corrected permeability, k_s^* , versus $\xi \bar{Kn}$ for $\varepsilon = 0.25, 0.4, 0.6$ and 0.8 ., keeping $\xi \bar{Kn}$ smaller than ~ 0.19 so that slip flow is expected to remain physically relevant. The apparent slip-corrected permeability was computed from the closure problem (3.7), on the one hand, and from (4.6) (i.e. from the solutions of problems (4.4) and (4.7)) for m up to 3, on the other hand. Figure 10 shows that the inaccuracy of the classical first-order approximation increases with $\xi \bar{Kn}$ and becomes much more significant while increasing ε .

For a more quantitative picture of the above, the relative error on the slip correction in k_s at the j th order, given by $(|k_s/k - 1 - \sum_{j=1}^m (\xi \bar{\lambda}_\beta)^j s_j|) / (k_s/k - 1) = (|k_s^* - k^*(1 + \sum_{j=1}^m (\xi \bar{\lambda}_\beta)^j s_j^*)|) / (k_s^* - k^*)$, is reported, up to the third order, versus $\xi \bar{Kn}$ in figure 11, for the four values of ε . When k_s is estimated at the first order, the relative error on the slip correction is $\sim 3.7\%$ for $\varepsilon = 0.25$ and $\xi \bar{Kn} \sim 0.19$ but reaches $\sim 20.3\%$ for $\varepsilon = 0.6$ and $\xi \bar{Kn} \sim 0.1$. The estimation of the slip correction is significantly improved while taking into account the second-order term, or further, the third-order term. In fact, for $m = 3$ and the structure under consideration, the relative error on the slip correction falls to approximately 0.6% for $\varepsilon = 0.25$ and $\xi \bar{Kn} \sim 0.19$ or 1.7% for $\varepsilon = 0.6$ and $\xi \bar{Kn} \sim 0.1$. This is clearly illustrated in figure 11. If a different Knudsen number, say \bar{Kn}_σ , based on the characteristic size, ℓ_σ , of the solid phase is used instead of \bar{Kn} , one would observe that the nonlinearity appears for $\xi \bar{Kn}_\sigma = \ell_\beta / \ell_\sigma \xi \bar{Kn} \simeq 0.02$, a value smaller than, or, when ε is large, almost equal to $\xi \bar{Kn}$, as ℓ_β / ℓ_σ takes the values 1.98×10^{-2} , 1.49×10^{-1} , 4.21×10^{-1} and 1.07 for $\varepsilon = 0.25, 0.4, 0.6$ and 0.8 respectively.

One must however be clear about the physical meaning of the macroscopic slip-correction terms for $j \geq 2$ obtained from the development leading to (4.10b). In fact, it must be kept in mind that the pore-scale physical model from which the macroscale balance equations derive involves a slip boundary condition and a momentum equation that are both first-order accurate in $\xi \bar{Kn}$. As a consequence, the macroscopic slip-correction terms beyond the first order in $\xi \bar{Kn}$ account for

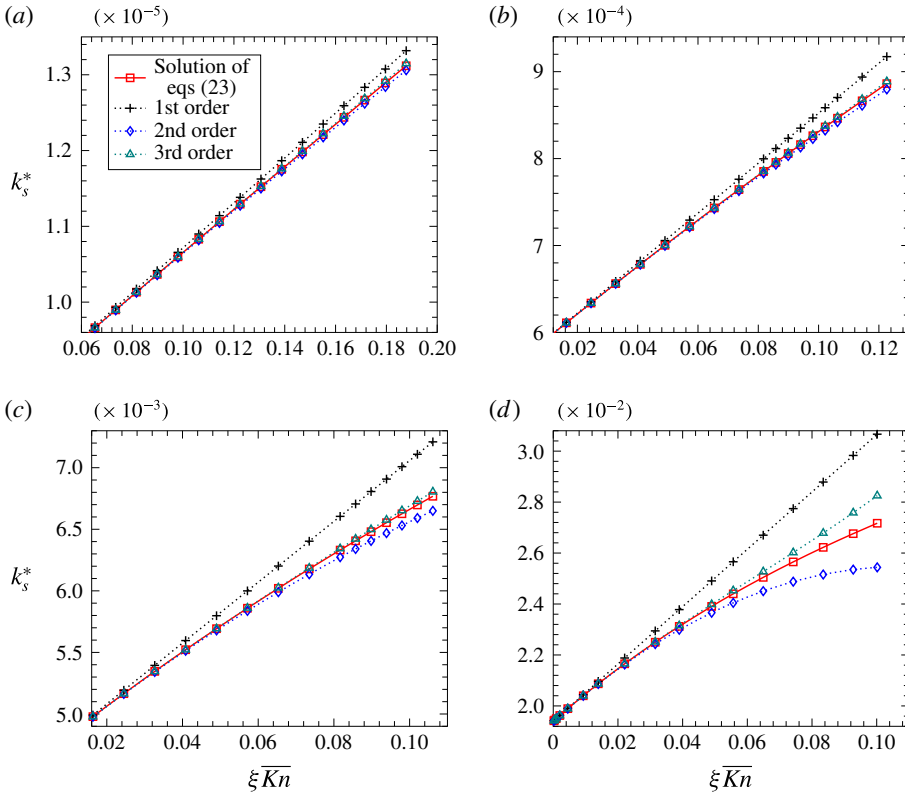


FIGURE 10. (Colour online) Comparison of the dimensionless apparent slip-corrected permeability, $k_s^* = k_s/\ell^2$, computed from the solution of the closure problem (3.7), on the one hand, and estimated at the first, second and third orders with (4.6) and the solutions of expanded closure problems (4.4) and (4.7), on the other hand. Periodic model structure of figure 2: (a) $\varepsilon = 0.25$; (b) $\varepsilon = 0.4$; (c) $\varepsilon = 0.6$; (d) $\varepsilon = 0.8$. Here \overline{Kn} is the macroscale Knudsen number based on the fluid-phase characteristic length scale: $\xi \overline{Kn} = \xi(\lambda_\beta/\ell_\beta)$.

the contribution of microstructural effects, i.e. the signature of pore topology on the averaged slip effect that can significantly depend upon local constrictions, enlargements and curvature of pore walls through the strain rate at $\mathcal{A}_{\beta\sigma}$. One can note, in particular, that the macroscopic model and associated closures provide an exact macroscopic solution in the case of slip flow in a bundle of straight capillary tubes or slits made of plane parallel plates. Indeed, this solution exactly corresponds to that obtained by averaging the pore-scale flow solution. In this situation with no curvature at the pore scale in the direction of the flow, which is 1-D, the macroscopic slip correction remains at the first order that is exactly obtained from the closure problem (4.7) for $j = 1$, all the higher-order closure problems yielding $\mathbf{D}_j = 0$ ($j \geq 2$). To be more precise, specific general properties of the slip boundary condition and the consequences on the closure problems are highlighted in the following section.

Before moving on, it is important to mention that some results obtained from a numerical solution of an approximate version of the Boltzmann equations (i.e. Bhatnagar Gross and Krook (BGK) model) under a linearized approach, predict a linear dependence of the apparent permeability with the Knudsen number over the whole range of $\xi \overline{Kn}$ investigated here for $\varepsilon = 0.8$ (these results were provided by an

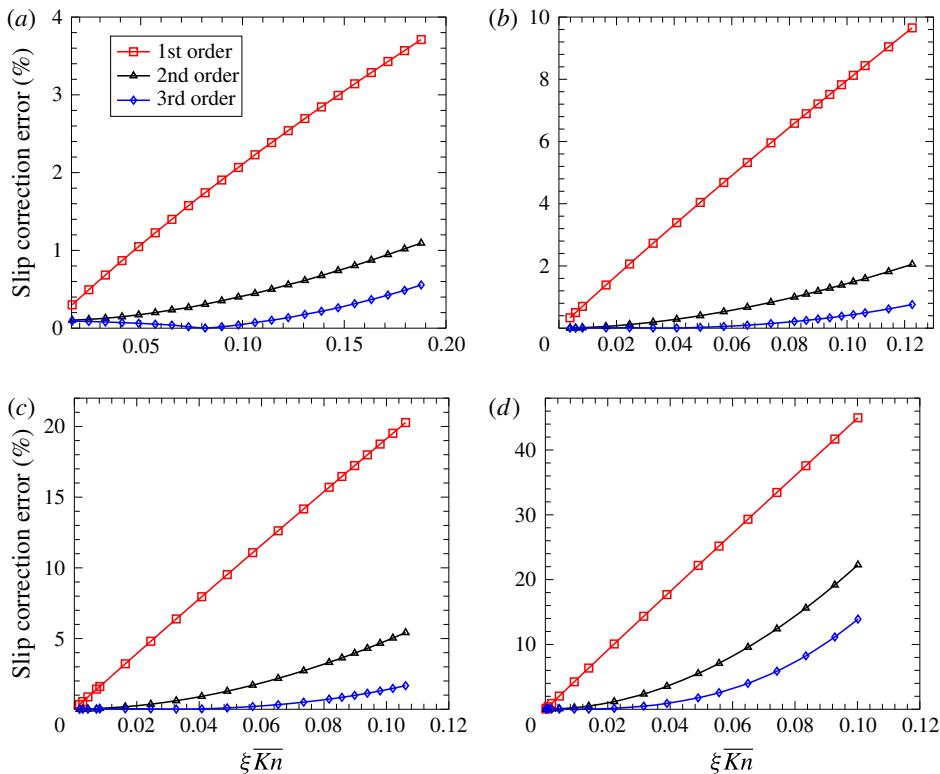


FIGURE 11. (Colour online) Relative error on the slip-flow correction in k_s estimated at the first, second and third orders taking the slip correction extracted from k_s computed from the solution of the closure problem (3.7) as the reference (see complete expression in the text). Periodic model structure of figure 2: (a) $\varepsilon = 0.25$; (b) $\varepsilon = 0.4$; (c) $\varepsilon = 0.6$; (d) $\varepsilon = 0.8$.

anonymous reviewer and are available from the authors). The contrast with the present results would suggest that the range of application of the slip-flow model should be drastically reduced as the porosity increases. This result is however difficult to justify physically. Moreover, the linear dependence of k_s^* with the Knudsen number resulting from this linearized BGK approach seems to hold for Knudsen number values up to approximately 0.5, fitting the predictions of Chang’s unit cell solution that is however expanded at the first order in the limit of $\xi \bar{Kn} \ll 1$; the reason for such a surprising behaviour remains unclear. Some possible sources for explaining this linear behaviour are the use of a linearized BGK model, along with the numerical method used to solve it.

The above remarks should not be considered as a definitive argument to accept a nonlinear dependence of the apparent permeability with the Knudsen number. In this regard, the finding of this behaviour should motivate the performance of slightly compressible rarefied gas flow experiments in highly permeable porous media.

4.3. Some important features of the slip boundary condition

An incomplete slip boundary condition, in which the $\nabla \mathbf{v}_\beta^T$ term has been dropped, has often been used for porous media flow (Skjetne & Auriault 1999; Pavan & Chastanet 2011), and we have shown, in accordance with some previous references

(Barber *et al.* 2004; Lockerby *et al.* 2004; Panzer *et al.* 1992), that this physically unjustified form can lead to a significant error in some circumstances (see § 3.3). Together with the nonlinear dependence of the slip correction on $\xi \overline{Kn}$, this suggests a close attention to the slip-like boundary condition of (4.7c) in the j th-order closure problem.

The analysis starts with an alternative expression of the second term on the right-hand side of (4.7c) given by

$$\begin{aligned}
 (\mathbf{I} - \mathbf{nn}) \cdot (\mathbf{n} \cdot (\nabla \mathbf{D}_{j-1})^{T1}) &= (\mathbf{I} - \mathbf{nn}) \cdot \nabla (\mathbf{n} \cdot \mathbf{D}_{j-1}) \\
 &\quad - (\mathbf{I} - \mathbf{nn}) \cdot (\nabla \mathbf{n} \cdot \mathbf{D}_{j-1}) \quad \text{at } \mathcal{A}_{\beta\sigma}. \tag{4.11}
 \end{aligned}$$

For all j , $\mathbf{n} \cdot \mathbf{D}_{j-1} = 0$ at $\mathcal{A}_{\beta\sigma}$ since \mathbf{D}_{j-1} is either 0 ($j = 1$) or purely tangential to $\mathcal{A}_{\beta\sigma}$ at this interface ($j \geq 2$). Consequently, $\nabla (\mathbf{n} \cdot \mathbf{D}_{j-1})$ is purely normal to $\mathcal{A}_{\beta\sigma}$ and this allows rewriting (4.11) as

$$(\mathbf{I} - \mathbf{nn}) \cdot (\mathbf{n} \cdot (\nabla \mathbf{D}_{j-1})^{T1}) = -\nabla_s \mathbf{n} \cdot \mathbf{D}_{j-1} \quad \text{at } \mathcal{A}_{\beta\sigma}, \tag{4.12}$$

where ∇_s denotes the surface differentiation operator defined by $\nabla_s \equiv (\mathbf{I} - \mathbf{nn}) \cdot \nabla$.

For $j = 1$, this result can be further simplified due to the no-slip boundary condition on \mathbf{D}_0 (see (4.4c)) leading to

$$(\mathbf{I} - \mathbf{nn}) \cdot (\mathbf{n} \cdot (\nabla \mathbf{D}_0)^{T1}) = 0 \quad \text{at } \mathcal{A}_{\beta\sigma} \tag{4.13}$$

and this proves that the $\nabla \mathbf{v}_\beta^T$ term in the slip boundary condition does not play any role up to the first order of the expansion in $\xi \overline{Kn}$ at the closure level. At higher orders, (4.12) cannot be further simplified and indicates that the contribution of $(\mathbf{I} - \mathbf{nn}) \cdot (\mathbf{n} \cdot (\nabla \mathbf{D}_{j-1})^{T1})$ depends on $\nabla_s \mathbf{n}$ that is related to the curvature of $\mathcal{A}_{\beta\sigma}$. In 2-D, for instance, it can be easily demonstrated (see appendix B) that $\nabla_s \mathbf{n} = -\kappa (\mathbf{I} - \mathbf{nn})$ where $\kappa = -\nabla_s \cdot \mathbf{n}$ is exactly the curvature of $\mathcal{A}_{\beta\sigma}$. This clearly shows that the $(\nabla \mathbf{D}_{j-1})^{T1}$ term does play a role in the slip-like boundary condition (4.7c) of the closure problem at the j th order, $j \geq 2$, in the general case. Its contribution vanishes only in some special geometrical situations where the flow is 1-D and the curvature of $\mathcal{A}_{\beta\sigma}$ is zero in the flow direction. This last remark applies to the boundary condition of (2.1d) at the pore scale and justifies why the incomplete form of the slip boundary condition can be used in the case of straight tubes, slits or channels that have been extensively used for the study of Knudsen effects in the slip regime (Fishman & Hetsroni 2005; Lauga & Cossu 2005; Shen *et al.* 2007).

The analysis is pursued with an alternative expression of the first term on the right-hand side of (4.7c), which can be written as

$$(\mathbf{I} - \mathbf{nn}) \cdot (\mathbf{n} \cdot \nabla \mathbf{D}_{j-1}) = \nabla_s \cdot (\mathbf{n} \mathbf{D}_{j-1}) + \kappa \mathbf{D}_{j-1} \quad \text{at } \mathcal{A}_{\beta\sigma}. \tag{4.14}$$

This finally allows us to express the slip-like boundary condition in (4.7c) for the j th-order closure problem as

$$\mathbf{D}_j = -\nabla_s \cdot (\mathbf{n} \mathbf{D}_{j-1}) + (\nabla_s \mathbf{n} - \kappa \mathbf{I}) \cdot \mathbf{D}_{j-1} \quad \text{at } \mathcal{A}_{\beta\sigma}. \tag{4.15}$$

In 2-D, this last expression takes the form $\mathbf{D}_j = -\nabla_s \cdot (\mathbf{n} \mathbf{D}_{j-1}) - 2\kappa \mathbf{D}_{j-1}$. For $j = 1$, it simplifies to

$$\mathbf{D}_1 = -(\mathbf{I} - \mathbf{nn}) \cdot (\mathbf{n} \cdot \nabla \mathbf{D}_0) = -\nabla_s \cdot (\mathbf{n} \mathbf{D}_0) \quad \text{at } \mathcal{A}_{\beta\sigma}. \tag{4.16}$$

Equations (4.15) and (4.16) show that the slip-like boundary condition in the j th-order closure problem contains an explicit dependence on the curvature of $\mathcal{A}_{\beta\sigma}$ that is however filtered out at the first order in $\xi\overline{Kn}$. This explains why the classical first-order macroscopic slip-flow model remains inaccurate for systems presenting a significant curvature of the solid–fluid interface. For the periodic square pattern of circular cylinders, it clearly justifies why the error on the slip correction, when restricted to the first order, increases with the porosity, as curvature scales as $(1 - \varepsilon)^{-1/2}$ in that case. This also justifies the necessity of taking into account higher-order terms in the macroscopic model as in (4.10b).

Finally, it must be noted that the analysis carried out in this section may be straightforwardly applied to an expansion in the Knudsen number performed on the original initial boundary value problem given in (2.1). In that way, the slip boundary condition properties at the successive orders in Kn may be generalized far beyond the strict context of porous media flow, i.e. for any situation allowing such an expansion in Kn .

5. Conclusion

Macroscopic modelling of slightly compressible gas slip flow in homogeneous porous media was thoroughly revisited and several important results were highlighted.

Under a specified set of constraints, the macroscopic model was shown to have a Darcy-like form in which the apparent non-intrinsic slip-corrected permeability tensor is given by a non-intrinsic closure problem having the structure of an incompressible Stokes flow problem with a slip-like boundary condition. The validity of the macroscopic model and associated closure was verified through comparisons with analytic solutions and DNS on model porous structures. The apparent slip-corrected permeability was shown to be a non-symmetric tensor in the general case, whereas a sufficient condition for quasi-symmetry to occur was derived. A nonlinear dependence of the apparent slip-corrected permeability on the averaged Knudsen number was evidenced that can become increasingly significant while increasing the porosity and the Knudsen number on the model structure under concern.

A reformulation of the macroscopic model and closure was derived using an expansion of the closure variables in the Knudsen number. This reformulation identifies the viscous and slip contributions that are, otherwise, lumped together in the apparent slip-corrected permeability. To the 0th order, the macroscopic model corresponds to the classical flow problem without slip, the associated macroscopic coefficient being the intrinsic permeability tensor. The successive higher-order terms in the macroscopic model are characterized by intrinsic slip-flow correction tensors that are all determined by easy-to-solve intrinsic closure problems that have basically the same Stokes structure and are coupled to each other and to the 0th-order closure problem through their slip-like boundary condition. The first-order correction was found to be in excellent agreement with a previous existing and validated model (Lasseux *et al.* 2014). Higher-order corrections account for the nonlinear behaviour of the apparent slip-corrected permeability versus the Knudsen number observed previously. Correction beyond the first order must be understood as a signature of pure geometrical effects of the microstructure, through the strain rate at the solid–fluid interface involved in the microscale slip boundary condition which is sensitive to local interface curvatures. Within a simple model structure, at large values of the porosity, errors of up to 45 % on the slip correction were found when restricted to an estimation at the first order.

The closure problem providing the first-order slip correction was shown to be insensitive to an incomplete slip-flow boundary condition where the ∇v_β^T term is omitted and that has been often abusively used in the statement of the pore-scale physical problem as reported in many references (Skjetne & Auriault 1999; Pavan & Chastanet 2011). This result does not hold for higher-order slip-correction terms. Moreover, it was shown that the explicit dependence of the slip-like boundary condition on the curvature of solid–fluid interfaces is filtered out at the closure level when the model is restricted to a first-order approximation, explaining the inaccuracy of the existing model reported in the literature and justifying the importance of higher-order slip-correction terms. This is an important general feature of the slip boundary condition, that applies beyond the context of porous media flow, providing a new physical insight into slip flow.

Supplementary work is needed for a further comparison of the present investigation with experimental data in particular for highly porous structures.

Acknowledgements

FVP expresses his gratitude to Fondo Sectorial de Investigación para la educación from CONACyT (Project number: 12511908; Arrangement number: 112087) for the financial aid provided. Authors are thankful to L. Mieussens, B. Dubroca, S. Brull and P. Charrier from University of Bordeaux for fruitful discussions about the BGK method. Special thanks are due to an anonymous reviewer who brought to our attention the results obtained from this numerical approach.

Appendix A

In this appendix, the symmetry properties of the apparent slip-corrected permeability tensor, \mathbf{K}_s , in the Darcy-like form of the macroscopic momentum equation (3.13b), are analysed. This apparent permeability is explicitly given by the closure problem (3.7)

$$\nabla \cdot \mathbf{D} = 0 \quad \text{in } \mathcal{V}_\beta \quad (\text{A } 1a)$$

$$0 = -\nabla d + \nabla^2 \mathbf{D} + \mathbf{I} \quad \text{in } \mathcal{V}_\beta \quad (\text{A } 1b)$$

$$\mathbf{D} = -\xi \bar{\lambda}_\beta (\mathbf{I} - \mathbf{nn}) \cdot (\mathbf{n} \cdot (\nabla \mathbf{D} + (\nabla \mathbf{D})^{T1})) \quad \text{at } \mathcal{A}_{\beta\sigma} \quad (\text{A } 1c)$$

$$\langle \mathbf{d} \rangle^\beta = 0 \quad (\text{A } 1d)$$

$$\langle \mathbf{D} \rangle = \mathbf{K}_s \quad (\text{A } 1e)$$

$$\begin{aligned} \text{Periodicity } \mathbf{D}(\mathbf{r} + \mathbf{l}_i) &= \mathbf{D}(\mathbf{r}), \\ \mathbf{d}(\mathbf{r} + \mathbf{l}_i) &= \mathbf{d}(\mathbf{r}), \quad i = 1, 2, 3. \end{aligned} \quad (\text{A } 1f)$$

The analysis starts with a pre-multiplication of (A 1b) by \mathbf{D}^T and when the superficial average of the result is formed, one obtains

$$0 = -\langle \mathbf{D}^T \cdot \nabla d \rangle + \langle \mathbf{D}^T \cdot \nabla^2 \mathbf{D} \rangle + \mathbf{K}_s^T. \quad (\text{A } 2)$$

The first term on the right-hand side of the above equation can be equivalently expressed as

$$\langle \mathbf{D}^T \cdot \nabla d \rangle = \langle \nabla \cdot (\mathbf{D}d) \rangle - \langle (\nabla \cdot \mathbf{D})d \rangle \quad (\text{A } 3)$$

and, since \mathbf{D} is a divergence-free tensor as stated in (A 1a), this is equivalent to

$$\langle \mathbf{D}^T \cdot \nabla d \rangle = \langle \nabla \cdot (\mathbf{D}d) \rangle. \quad (\text{A } 4)$$

Making use of the averaging theorem (see (2.8)) in its divergence form, one obtains

$$\langle \mathbf{D}^T \cdot \nabla \mathbf{d} \rangle = \nabla \cdot \langle \mathbf{D} \mathbf{d} \rangle + \frac{1}{V} \int_{\mathcal{A}_{\beta\sigma}} \mathbf{n} \cdot \mathbf{D} \mathbf{d} \, dA. \tag{A 5}$$

Because \mathbf{D} and \mathbf{d} are periodic

$$\nabla \cdot \langle \mathbf{D} \mathbf{d} \rangle = 0 \tag{A 6}$$

and, since \mathbf{D} has no normal component at $\mathcal{A}_{\beta\sigma}$ as indicated by the boundary condition in (A 1c),

$$\mathbf{n} \cdot \mathbf{D} = 0 \quad \text{at } \mathcal{A}_{\beta\sigma}. \tag{A 7}$$

From (A 5), it follows that

$$\langle \mathbf{D}^T \cdot \nabla \mathbf{d} \rangle = 0. \tag{A 8}$$

Returning to equation (A 2), we hence have

$$0 = \langle \mathbf{D}^T \cdot \nabla^2 \mathbf{D} \rangle + \mathbf{K}_s^T. \tag{A 9}$$

The first term on the right-hand side of this last relationship can be rewritten as

$$\langle \mathbf{D}^T \cdot \nabla^2 \mathbf{D} \rangle = \langle \nabla^2 (\mathbf{D}^T) \cdot \mathbf{D} \rangle^T \tag{A 10}$$

in which we have used the trivial property $(\nabla^2 \mathbf{D})^T = \nabla^2 (\mathbf{D}^T)$. Equation (A 10) can be arranged according to the fact that, for any two second-order tensors \mathbf{A} and \mathbf{B} , $\nabla^2 \mathbf{A} \cdot \mathbf{B} = \nabla \cdot (\nabla \mathbf{A} \cdot \mathbf{B}) - (\nabla \mathbf{A})^{T1} : (\nabla \mathbf{B})^{T1}$ and, when \mathbf{A} is identified to \mathbf{D}^T and \mathbf{B} to \mathbf{D} , this yields

$$\langle \mathbf{D}^T \cdot \nabla^2 \mathbf{D} \rangle = \langle \nabla \cdot (\nabla (\mathbf{D}^T) \cdot \mathbf{D}) \rangle^T - \langle (\nabla \mathbf{D}^T)^{T1} : (\nabla \mathbf{D})^{T1} \rangle^T. \tag{A 11}$$

In the above expressions, we have used the superscript $T1$ to designate the transpose of a third-order tensor that permutes the two first indices and we adopted the classical nested convention for double dot product. The last equation can be equivalently written as

$$\langle \mathbf{D}^T \cdot \nabla^2 \mathbf{D} \rangle = \langle \nabla \cdot (\nabla (\mathbf{D}^T) \cdot \mathbf{D}) \rangle^T - \langle (\nabla \mathbf{D})^{T3} : \nabla \mathbf{D} \rangle^T, \tag{A 12}$$

where the superscript $T3$ denotes the transpose of a third-order tensor that permutes the first and third indices. When this result is inserted back into (A 9), we have

$$0 = \langle \nabla \cdot (\nabla (\mathbf{D}^T) \cdot \mathbf{D}) \rangle - \langle (\nabla \mathbf{D})^{T3} : \nabla \mathbf{D} \rangle + \mathbf{K}_s. \tag{A 13}$$

The attention is now focused on the first term on the right-hand side of the last relationship, which, upon use of the averaging theorem, can be equivalently written as

$$\langle \nabla \cdot (\nabla (\mathbf{D}^T) \cdot \mathbf{D}) \rangle = \nabla \cdot \langle \nabla (\mathbf{D}^T) \cdot \mathbf{D} \rangle + \frac{1}{V} \int_{\mathcal{A}_{\beta\sigma}} \mathbf{n} \cdot \nabla (\mathbf{D}^T) \cdot \mathbf{D} \, dA. \tag{A 14}$$

Since \mathbf{D} is periodic, $\nabla(\mathbf{D}^T)$ is also periodic and hence

$$\nabla \cdot \langle \nabla(\mathbf{D}^T) \cdot \mathbf{D} \rangle = 0 \tag{A 15}$$

so that

$$\langle \nabla \cdot (\nabla(\mathbf{D}^T) \cdot \mathbf{D}) \rangle = \frac{1}{V} \int_{\mathcal{A}_{\beta\sigma}} \mathbf{n} \cdot \nabla(\mathbf{D}^T) \cdot \mathbf{D} \, dA. \tag{A 16}$$

We can now make use of the general identity

$$\mathbf{u} \cdot \nabla \mathbf{A} \cdot \mathbf{B} = (\nabla \mathbf{A})^{T1} : (\mathbf{u}\mathbf{B})^{T1} \tag{A 17}$$

valid for any two second-order tensors \mathbf{A} and \mathbf{B} and any vector \mathbf{u} , and when \mathbf{A} is identified to \mathbf{D}^T , \mathbf{B} to \mathbf{D} and \mathbf{u} to \mathbf{n} , this provides an alternative form of the interfacial integral term on the right-hand side of (A 16). When replaced in (A 13), the apparent slip-corrected permeability, \mathbf{K}_s , can finally be recast into the following expression

$$\mathbf{K}_s = \langle (\nabla \mathbf{D})^{T3} : \nabla \mathbf{D} \rangle - \frac{1}{V} \int_{\mathcal{A}_{\beta\sigma}} (\nabla \mathbf{D})^{T3} : (\mathbf{n}\mathbf{D}) \, dA. \tag{A 18}$$

While the tensor $\langle (\nabla \mathbf{D})^{T3} : \nabla \mathbf{D} \rangle$ in this expression can be easily shown to be symmetric, the tensor represented in the area average term is not symmetric in the general case, except if the interface $\mathcal{A}_{\beta\sigma}$ has specific symmetry properties. This is the case, for example, of an ordered porous structure for which the solid σ -phase exhibits symmetries about the three planes parallel to the edges of the periodic unit cell and passing through its centroid. In such circumstances, the off-diagonal terms of \mathbf{K}_s are all zero. The expression of \mathbf{K}_s in (A 18) shows that this tensor is generally not symmetric (Skjetne & Auriault 1999).

The investigation can be further pursued by examining the condition under which \mathbf{K}_s is close to a symmetric tensor. A sufficient condition is when the non-symmetric part in (A 18) remains small compared to the symmetric part and this can be expressed in terms of the orders of magnitude of these two respective terms as

$$O \left(\frac{1}{V} \int_{\mathcal{A}_{\beta\sigma}} (\nabla \mathbf{D})^{T3} : (\mathbf{n}\mathbf{D}) \, dA \right) \ll O(\langle (\nabla \mathbf{D})^{T3} : \nabla \mathbf{D} \rangle). \tag{A 19}$$

By making use of the boundary condition in (A 1c), the above constraint can be expressed as

$$O \left(\xi \bar{\lambda}_\beta \frac{1}{V} \int_{\mathcal{A}_{\beta\sigma}} (\mathbf{n}(\mathbf{I} - \mathbf{nn}) \cdot (\mathbf{n} \cdot (\nabla \mathbf{D} + (\nabla \mathbf{D})^{T1}))) : (\nabla \mathbf{D})^{T3} \, dA \right) \ll O(\langle (\nabla \mathbf{D})^{T3} : \nabla \mathbf{D} \rangle). \tag{A 20}$$

The order of magnitude of the area average can be estimated to be

$$\xi \bar{\lambda}_\beta \frac{1}{V} \int_{\mathcal{A}_{\beta\sigma}} (\mathbf{n}(\mathbf{I} - \mathbf{nn}) \cdot (\mathbf{n} \cdot (\nabla \mathbf{D} + (\nabla \mathbf{D})^{T1}))) : (\nabla \mathbf{D})^{T3} \, dA = \xi \bar{\lambda}_\beta O \left(a_v \frac{D^2}{\ell_\beta^2} \right), \tag{A 21}$$

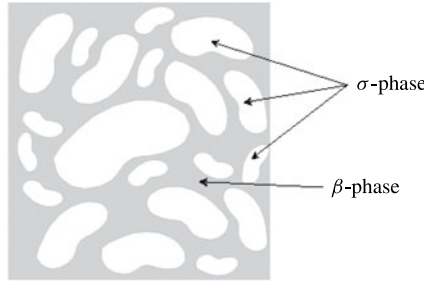


FIGURE 12. Unit cell for the computation of the full apparent slip-corrected permeability tensor. $\varepsilon \simeq 0.515$, $a_v^* \simeq 11.935$.

where D denotes the leading order of the components of \mathbf{D} . Similarly, the symmetric part can be estimated according to

$$\langle (\nabla \mathbf{D})^{T3} : \nabla \mathbf{D} \rangle = \mathcal{O} \left(\varepsilon \frac{D^2}{\ell_\beta^2} \right). \tag{A 22}$$

These two estimates allow us to formulate the constraint (A 20) as

$$\xi \bar{\lambda}_\beta \ll \mathcal{O} \left(\frac{\varepsilon}{a_v} \right). \tag{A 23}$$

If a_v is thought to vary as ℓ_β^{-1} as is often accepted (Whitaker 1999), one would be left with

$$\xi \bar{K}n \ll \mathcal{O}(\varepsilon) \tag{A 24}$$

as a sufficient condition for \mathbf{K}_s to remain quasi-symmetric. It should be noted that this is consistent with the fact that, when no slip occurs, corresponding to $\bar{K}n \simeq 0$, $\mathbf{K}_s = \mathbf{K}$, which is a symmetric tensor as predicted by (A 18) when $\xi \bar{\lambda}_\beta = 0$, i.e. when $\mathbf{D} = 0$ at $\mathcal{A}_{\beta\sigma}$.

A short illustration of the symmetry properties can be provided from direct computation of \mathbf{K}_s over a unit cell that does not possess any particular geometrical symmetry as the one represented in figure 12 for which $\varepsilon \simeq 0.515$ and $a_v^* = a_v \ell \simeq 11.935$. The apparent slip-corrected permeability was determined from the solution of the closure problem of (A 1) above and for a cell Knudsen number, $\xi \bar{\lambda}_\beta^* = \xi \bar{\lambda}_\beta / \ell$, ranging from 10^{-4} to 1.

Results on the components of $\mathbf{K}_s^* = \mathbf{K}_s / \ell^2$, reported in table 2, clearly show that the contrast between the off-diagonal terms of \mathbf{K}_s^* remains small when the constraint expressed in (A 23), $\xi \bar{\lambda}_\beta^* \ll \mathcal{O}(\varepsilon / a_v^* \simeq 0.043)$, is satisfied and becomes very significant otherwise.

Appendix B

The objective of this appendix is to demonstrate that, in the 2-D case and with the notations used throughout the paper,

$$\nabla_s \mathbf{n} = -\kappa (\mathbf{I} - \mathbf{nn}), \tag{B 1}$$

$\xi \bar{\lambda}_\beta^*$	k_{xxx}^*	k_{syx}^*	k_{sxy}^*	k_{syy}^*	$2 \frac{ k_{syx}^* - k_{sxy}^* }{(k_{syx}^* + k_{sxy}^*)} (\%)$
1.00 10^{-4}	1.26 10^{-4}	5.87 10^{-6}	5.80 10^{-6}	9.28 10^{-5}	1.15
0.01	2.13 10^{-4}	6.87 10^{-6}	9.09 10^{-6}	1.59 10^{-4}	27.80
0.10	4.95 10^{-4}	6.91 10^{-6}	1.57 10^{-5}	3.40 10^{-4}	78.00
1.00	7.24 10^{-4}	5.82 10^{-6}	1.87 10^{-5}	4.62 10^{-4}	105.00

TABLE 2. Components of the dimensionless apparent slip-corrected permeability tensor for the unit cell of figure 12 and four values of $\xi \bar{\lambda}_\beta^*$. The contrast between k_{syx}^* and k_{sxy}^* is estimated in the last column.

where $\kappa = -\nabla_s \cdot \mathbf{n}$ is the curvature of $\mathcal{A}_{\beta\sigma}$ and ∇_s the surface differentiation operator defined by $\nabla_s \equiv (\mathbf{I} - \mathbf{nn}) \cdot \nabla$.

We shall start by noticing that, since \mathbf{n} is a unit vector, $\mathbf{n} \cdot \mathbf{n} = 1$ and hence $\nabla(\mathbf{n} \cdot \mathbf{n}) = 0$, which leads to the straightforward relationship

$$\nabla \mathbf{n} \cdot \mathbf{n} = 0. \tag{B 2}$$

When this result is employed in the expression of the product $(\mathbf{I} - \mathbf{nn}) \cdot \nabla \mathbf{n}$, along with the fact that \mathbf{n} is a unit vector, one ends up with

$$\nabla_s \mathbf{n} = (\mathbf{I} - \mathbf{nn}) \nabla \cdot \mathbf{n} \tag{B 3}$$

in the specific 2-D case.

Let us now consider the expression of the curvature in the general case (2-D or 3-D) and write $\nabla_s \cdot \mathbf{n}$ from its definition as

$$\nabla_s \cdot \mathbf{n} = ((\mathbf{I} - \mathbf{nn}) \cdot \nabla) \cdot \mathbf{n} = \nabla \cdot \mathbf{n} - (\mathbf{nn} \cdot \nabla) \cdot \mathbf{n}. \tag{B 4}$$

The last term in the right-hand side of (B 4) can be explicitly re-written as

$$((\mathbf{nn} \cdot \nabla) \cdot \mathbf{n})_{ij} = n_i n_j \frac{\partial n_i}{\partial x_j} = n_j (\nabla \mathbf{n})_{ji} n_i, \tag{B 5}$$

where we have implicitly used Einstein notation, and this means that

$$(\mathbf{nn} \cdot \nabla) \cdot \mathbf{n} = \mathbf{n} \cdot \nabla \mathbf{n} \cdot \mathbf{n}. \tag{B 6}$$

However, due to (B 2), the last result simplifies to

$$(\mathbf{nn} \cdot \nabla) \cdot \mathbf{n} = 0. \tag{B 7}$$

Coming back to (B 4), it follows that

$$\nabla_s \cdot \mathbf{n} = \nabla \cdot \mathbf{n} = -\kappa, \tag{B 8}$$

which leads to the expected relationship expressed in (B 1), valid in 2-D, when the result of (B 3) is taken into account.

REFERENCES

- AGRAWAL, A. & PRABHU, S. V. 2008 Survey on measurement of tangential momentum accommodation coefficient. *J. Vac. Sci. Technol. A* **26**, 634–645.
- ARKILIC, E. B., BREUER, K. S. & SCHMIDT, M. A. 2001 Mass flow and tangential momentum accommodation in silicon micromachined channels. *J. Fluid Mech.* **437**, 29–43.
- BARBER, R. W., SUN, Y., GU, X. J. & EMERSON, D. R. 2004 Isothermal slip flow over curved surfaces. *Vacuum* **76**, 73–81.
- BARRÈRE, J., GIPOULOUX, O. & WHITAKER, S. 1992 On the closure problem for Darcy's law. *Trans. Porous Med.* **7**, 209–222.
- BRUSCHKE, M. V. & ADVANI, S. G. 1993 Flow of generalized Newtonian fluids across a periodic array of cylinders. *J. Rheol.* **37**, 479–498.
- CAI, C., SUN, Q. & BOYD, I. D. 2007 Gas flows in microchannels and microtubes. *J. Fluid Mech.* **589**, 305–314.
- CHAI, Z., LU, J., SHI, B. & GUO, Z. 2011 Gas slippage effect on the permeability of circular cylinders in a square array. *Int. J. Heat Mass Transfer* **54**, 3009–3014.
- CHMIELEWSKI, R. D. & GOREN, S. L. 1972 Aerosol filtration with slip flow. *Environ. Sci. Technol.* **6** (13), 1101–1105.
- COWLING, T. G. 1950 *Molecules in Motion*, chap. IV. Hutchinson.
- DARABI, H., ETTEHAD, A., JAVADPOUR, F. & SEPEHRNOORI, K. 2012 Gas flow in ultra-tight shale strata. *J. Fluid Mech.* **710**, 641–658.
- DESOCIO, L. M. & MARINO, L. 2006 Gas flow in a permeable medium. *J. Fluid Mech.* **557**, 119–133.
- EINZEL, D., PANZER, P. & LIU, M. 1990 Boundary condition for fluid flow: curved or rough surfaces. *Phys. Rev. Lett.* **64** (19), 2269–2272.
- FISHMAN, M. & HETSRONI, G. 2005 Viscosity and slip velocity in gas flow in microchannels. *Phys. Fluids* **17**, 123102.
- GHADDAR, C. K. 1995 On the permeability of unidirectional fibrous media: a parallel computational approach. *Phys. Fluids* **7** (11), 2563–2586.
- GRAY, W. G. 1975 A derivation of the equations for multiphase transport. *Chem. Engng Sci.* **30**, 229–233.
- HARLEY, J. C., HUANG, Y., BAU, H. H. & ZEMEL, J. N. 1995 Gas flow in micro-channels. *J. Fluid Mech.* **284**, 257–274.
- HOWES, F. & WHITAKER, S. 1985 The spatial averaging theorem revisited. *Chem. Engng Sci.* **40**, 1387–1392.
- JANNOT, Y. & LASSEUX, D. 2012 A new method to measure gas permeability of weakly permeable porous media. *Rev. Sci. Instrum.* **83** (1), 015113.
- KARNIADAKIS, G. E., BESKOK, A. & ALURU, N. 2005 *Microflows and nanoflows. Fundamentals and Simulation*. Springer.
- KLINKENBERG, L. J. 1941 The permeability of porous media to liquids and gases. *API Drilling and Production Practice* pp. 200–213. Available at: <https://www.onepetro.org/conferences/API/API41>.
- KUWABARA, S. 1959 The forces experienced by randomly distributed parallel circular cylinders or spheres in a viscous flow at small Reynolds numbers. *J. Phys. Soc. Japan* **14** (4), 527–532.
- LASSEUX, D., JOLLY, P., JANNOT, Y., SAUGER, E. & OMNES, B. 2011 Permeability measurement of graphite compression packings. *Trans. ASME J: J. Press. Vessel Technol.* **133** (4), 041401.
- LASSEUX, D., VALDES PARADA, F. J., OCHOA TAPIA, J. A. & GOYEAU, B. 2014 A macroscopic model for slightly compressible gas slip-flow in homogeneous porous media. *Phys. Fluids* **26** (5), 053102.
- LAUGA, E. & COSSU, C. 2005 A note on the stability of slip channel flows. *Phys. Fluids* **17**, 088106.
- LOCKERBY, D. A., REESE, J. M., EMERSON, D. R. & BARBER, R. W. 2004 Velocity boundary condition at solid walls in rarefied gas calculations. *Phys. Rev. E* **70**, 017303.
- MAURER, J., TABELING, P., JOSEPH, P. & WILLAIME, H. 2003 Second-order slip laws in microchannels for helium and nitrogen. *Phys. Fluids* **15** (9), 2613–2621.

- MAXWELL, J. C. 1879 On stresses in rarefied gases arising from inequalities of temperature. *Phil. Trans. R. Soc. Lond.* **170**, 231–256.
- NAKASHIMA, Y. & WATANABE, Y. 2002 Estimate of transport properties of porous media by microfocus X-ray computed tomography and random walk simulation. *Water Resour. Res.* **38** (12), 1272.
- PANZER, P., LIU, M. & EINZEL, D. 1992 The effect of boundary curvature on hydrodynamic fluid flow: calculation of slip length. *Intl J. Mod. Phys. B* **06** (20), 3251–3278.
- PAVAN, V. & CHASTANET, J. 2011 Gas/solid heat transfer in gas flows under Klinkenberg conditions: comparison between the homogenization and the kinetic approaches. *J. Porous Media* **14**, 127–148.
- PERRIER, P., GRAUR, I. A., EWART, T. & MOLANS, J. G. 2011 Mass flow rate measurements in microtubes: From hydrodynamic to near free molecular regime. *Phys. Fluids* **23**, 042004.
- PORODNOV, B. T., SUETIN, P. E., BORISOV, S. F. & AKINSHIN, V. D. 1974 Experimental investigation of rarefied gas flow in different channels. *J. Fluid Mech.* **64** (3), 417–437.
- PRODANOVIĆ, M., LINDQUIST, W. B. & SERIGHT, R. S. 2007 3D image-based characterization of fluid displacement in a Berea core. *Adv. Water Resour.* **30**, 214–226.
- PROFICE, S., LASSEUX, D., JANNOT, Y., JEBARA, N. & HAMON, G. 2012 Permeability, porosity and Klinkenberg coefficient determination on crushed porous media. *Petrophysics* **53**, 430–438.
- SELDEN, N., GIMELSHEIN, N., GIMELSHEIN, S. & KETSDEVER, A. 2009 Analysis of accommodation coefficients of noble gases on aluminum surface with an experimental/computational method. *Phys. Fluids* **21**, 073101.
- SHEN, S., CHEN, G., CRONE, R. M. & ANAYA-DUFRESNE, M. 2007 A kinetic theory based first-order slip boundary condition for gas flow. *Phys. Fluids* **19**, 086101.
- SKJETNE, E. & AURIAULT, J. L. 1999 Homogenization of wall-slip gas flow through porous media. *Trans. Porous Med.* **36**, 293–306.
- SUETIN, P. E., PORODNOV, B. T., CHERNJAK, V. G. & BORISOV, S. F. 1973 Poiseuille flow at arbitrary Knudsen numbers and tangential momentum accommodation. *J. Fluid Mech.* **60** (3), 581–592.
- TRUESDELL, C. & TOUPIN, R. 1960 *The Classical Field Theories*. Springer.
- WHITAKER, S. 1999 *The Method of Volume Averaging, Theory and Applications of Transport in Porous Media*, vol. 13. Kluwer.
- ZHANG, T., ZHANG, P., LAW, C. K. & QI, F. 2009 CVD in weakly rarefied rotating disk flows. *Chem. Vapor Depos.* **15**, 274–280.